EFFECTS OF URBAN GROWTH ON TEMPORAL VARIATION OF SURFACE TEMPERATURE IN KATSINA METROPOLIS, NIGERIA

BY

JACOB, Reuben Jobien
MSC/SCI/05350/2011-2012
(REMOTE SENSING AND GIS)

BEING A THESIS SUBMITTED TO THE SCHOOL OF POSTGRADUATE STUDIES, AHMADU BELLO UNIVERSITY, ZARIA, IN PARTIAL FULFILLMENT OF THE REQUIREMENTS FOR THE AWARD OF MASTERS DEGREE IN GEOGRAPHY (REMOTE SENSING AND GEOGRAPHIC INFORMATION SYSTEM)

DEPARTMENT OF GEOGRAPHY, FACULTY OF SCIENCE, AHMADU BELLO UNIVERSITY, ZARIA NIGERIA

AUGUST, 2015

DECLARATION

I declare that the work in this thesis entitled Effects of Urban Growth on Temporal Variation of Surface Temperature in Katsina Metropolis, Nigeria has been performed by me in the Department of Geography. The information derived from the literature has been duly acknowledged in the text and a list of references provided. No part of this dissertation was previously presented for another degree or diploma at this or any other Institution.

Reuben Jobien JACOB	_____	_____
Name of Student	Signature	Date

CERTIFICATION

This dissertation entitled EFFECTS OF URBAN GROWTH ON TEMPORAL VARIATION OF SURFACE TEMPERATURE IN KATSINA METROPOLIS, NIGERIA by Reuben Jobien JACOB meets the regulations governing the award of Masters of Science Remote Sensing and Geographic Information System of the Ahmadu Bello University, and is approved for its contribution to knowledge and literary presentation.

Dr. B.A. Sawa Chairman, Supervisory Committee	_____ Signature	_____ Date
Dr. D.N. Jeb Member, Supervisory Committee	_____ Signature	_____ Date
Dr. I.M. Jaro Head of Department	_____ Signature	_____ Date
Prof. A.Z. Hassan Dean, School of Postgraduate Studies	_____ Signature	_____ Date

DEDICATION

This thesis is dedicated to my loving and caring mother Nancy Danchu, my brother Dominic Jacob and my sister Patience Jacob.

ACKNOWLEDGEMENT

I wish to express my profound gratitude to the chairman supervisory committee Dr. B.A. Sawa for his support and guidance throughout the period of this research work. Special thanks to the member of supervisory committee Dr. D.N. Jeb for his constructive criticisms and valuable suggestions.

I would also like to thank the Head of Department Dr. I.M. Jaro, the Post Graduate coordinator Dr. R.O. Yusuf and the Post Graduate seminar coordinator Dr. Obadaki for their their moral support.

I also wish to appreciate my lecturers and all the non teaching staff of the Department of Geography Ahmadu Bello University for their moral and academic support.

Finally, my appreciation goes to my classmates for their care and encouragement. Thank you very much.

ABSTRACT

Worldwide urbanization has significantly modified the radiative, thermal, moisture and aerodynamic characteristics of the landscape, which affect the surface energy balance within the atmosphere. Such modification can lead to urban heat island phenomenon where urban surface and air temperatures are higher than their corresponding rural areas. Remote sensing and GIS were used to evaluate the effect of urban growth on temporal variation of surface temperature in Katsina Metropolis. Landsat Thematic Mapper (TM), Enhanced Thematic Mapper Plus (ETM+) and Landsat-8 Operational Land imager (OLI) images of 1986, 1999 and 2014 respectively were utilized. Land use land cover maps were generated using supervised classification. The four (4) land use land cover classes identified in the study area are farmland, vegetation, bareland and built up. Thermal band data was used to compute surface temperature maps for the three years and the relationship between land use land cover and surface temperature was analyzed. Findings from this study revealed that there is a general decline in natural surfaces and increase in developed surfaces from 1986 to 2014. The resulting GIS analysis showed that built up is increasing at an annual average rate of 5.1 % while the Surface Temperature has gone up by more than 17^{o}C during the study period. If the built up continues to increase at the rate mentioned above and vegetation decline at an annual rate of 0.8%, Surface Temperature will be on the high side and this may bring about urban heat island. Therefore, planting of trees and vegetation in and around the metropolis should be encouraged to minimize the increase in surface temperatures of the land use/cover types which may also affects the mean surface temperature of Katsina metropolis.

Table of Contents

Title **Pages**

Title Page …….…….... i

Declaration ii

Certification ……..……..……...…… iii

Dedication iv

Acknowledgement v

Abstract vi

Table of Contents vii

List of Figures x

List of Tables xi

Abbreviations xii

CHAPTER ONE: INTRODUCTION

1.1 Background to the study 1

1.2 Statement of the Research Problem 4

1.3 Aim and Objectives of the Study 7

1.4 Scope of the Study 8

1.5 Justification of the Study 8

CHAPTER TWO: CONCEPTUAL FRAMEWORK AND LITERATURE REVIEW

2.1 Introduction 10

2.2 Conceptual Framework 10

2.2.1 Concept of Urbanization 10

2.2.2 Concept of Urban Heat Island 11

2.2.3 Relationship between Surface and Air Temperatures 12

2.2.4 Urban Heat Island Intensity 13

2.2.5 Urban surface energy balance 14

2.3 Literature Review 16

2.3.1 Urban Growth in Nigeria 16

2.3.2 Spatial Growth of Katsina Metropolis 17

2.3.3 Causes of Urban Growth 18

2.3.4 Consequences of Rapid Rate of Urban Growth 21

2.3.5 Thermal Remote Sensing of Urban Surface Temperature 23

2.3.6 Application of Remote Sensing and GIS in Urban Temperature Studies 26

2.3.7 Causes of Urban Heat Island 28

2.3.8 Effects of the Urban Heat Island 33

2.3.9 Mitigating the Urban Heat Island effect 38

CHAPTER THREE: THE STUDY AREA AND METHODOLOGY

3.1 Introduction 43

3.2 Study Area 43

3.2.1 Location 43

3.2.2 Climate 45

3.2.3 Hydrology 45

3.2.4 Landform 46

3.2.5 Geology 47

3.2.6 Soil 47

3.2.7 Vegetation..... 48

3.2.8 Population Structure and Distribution 49

3.2.9 Settlement 49

3.2.10 Land Uses 49

3.3 Methodology 51

3.3.1 Reconnaissance Survey 51

3.3.2 Types and Sources of Data 51

3.3.3 Hardware and Software 58

3.3.4 Methods of Data Analysis 58

CHAPTER FOUR: RESULTS AND DISCUSSIONS

4.1 Introduction 63

4.2 Land Use Land Cover Mapping 63

4.2.1 Land use Land Cover Classification 63

4.2.2 Accuracy Assessment of Image Classification 68

4.3 Land Use Land Cover Change 71

4.4 Surface Temperature Variation of Katsina Metropolis 73

4.5 Surface Temperature of Land Use Land Cover Types 75

CHAPTER 5: SUMMARY, CONCLUSSION AND RECOMMENDATION

5.1 Introduction 77

5.2 Summary 77

5.3 Conclusion 77

5.4 Recommendations 78

REFERENCES 79

LIST OF FIGURES

Fig 2.1 Differences between surface and air temperature during the day and at night...14

Fig 3.1 Map of the Study Area 44

Fig 4.1 1986 Land use Land Cover Classification map of the Study area 58

Fig 4.2 1999 Land use Land Cover Classification map of the Study area 59

Fig 4.3 2014 Land use Land Cover Classification map of the Study area 60

Fig 4.4 Surface Temperature Map of 1986, 1999 and 2014 68

LIST OF TABLES

Table 3.1 Satellite Image Information 52

Table 3.2 Classification Scheme 54

Table 3.3 Parameters for the Calculation of surface temperature 56

Table 4.1 Land use Land cover statistics 61

Table 4.2 Error matrix of 1986 Image Classification 62

Table 4.3 Error matrix of 1999 Image Classification 63

Table 4.4 Error matrix of 2014 Image Classification 64

Table 4.5 Land Use Land Cover Change Statistics 65

Table 4.6 Statistics of Surface Temperature 66

Table 4.7 Average Surface Temperature of Land use/cover types 69

ABBREVIATIONS

^{o}C	Degree Centigrade
^{o}F	Degree Fahrenheit
BLHI	Boundary Layer Heat Island
CLHI	Canopy Layer Heat Island
DN	Digital Number
e.g.	for example
et al.	and others
etc.	and the rest
EPA	Environmental Protection Agency
EROS	Earth Resources Observation and Science
ETM	Enhanced Thematic Mapper
ETM+	Enhanced Thematic Mapper
GIS	Geographic Information Science
GRA	Government Reserved Area
Ha	Hectare
ICAO	International Civil Aviation Organisation
i.e.	that is to say
ITD	Inter-Tropical Discontinuity
K	Temperature Kelvin
LGA	Local Government Area
LST	Land Surface Temperature
LULC	Land Use Land Cover
MS	Microsoft
NDBI	Normalized Difference Build-up Index

NDVI	Normalized Difference Vegetation Index
NOX	Nitrogen oxides
NTFPs	Non Timber Forest Products
O_3	Ozone
OLI	Operational Land Imager
ST	Surface Temperature
SUHI	Surface Urban Heat Island
TIRS	Thermal InfraRed Sensor
TM	Thematic Mapper
TOA	Top of the Atmosphere
UHI	Urban Heat Island
UN	United Nations
USGS	United States Geological Survey
UV	Ultraviolet
VOC	Volatile organic compound
WHO	World Health Organization

CHAPTER ONE: INTRODUCTION

1.1 BACKGROUND TO THE STUDY

Since 1950 there has been a huge worldwide increase in the percentage of population living within cities(Kaya, Basar, Karaca, & Seker, 2012). Approximately 59% of the world's population currently lives in urban areas, and this figure is further expected to increase especially in the developing countries where the fraction of the population that lives in cities is comparatively lower than the developed countries (Kaya *et al*, 2012). In the near future, it is expected that the global rate of urbanization will increase the world urban population up to 67% by 2030, as urban agglomerations emerge and population migration from rural to urban/suburban areas continue (Kaya, *et al*, 2012).

The last fifty years of the 20th century witnessed unprecedented urbanization in Nigeria. The rate of population growth has been spectacular in recent times. Compared to growth rate of 2.8 per cent annually for the total population, the urban population in Nigeria according to Alkali (2005) over the last three decades has been growing close to 5.8 per cent per annum. In fact the population of the urban centres in Nigeria constitute about 48.2 per cent of the country's total population and projections indicate that more than 60 per cent will live in urban centres by year 2025 (Alkali, 2005). Studies have shown that there are more than 840 urban centres and more than 10 cities with populations of over a million (Ayedun, Durodola & Akinjare, 2011).

In Katsina metropolis, land use and land cover patterns have undergone a rapid change due to accelerated expansion over the years. Urban growth has increased tremendously and extreme stress to the environment has occurred. Katsina has been growing rapidly owing to favourable socio-economic, political, and physical factors. The political change in the city's status as a result of the creation of Katsina state by the Federal Government of Nigeria in the late 1987, and the

making of Katsina town the state's capital, is viewed as the principal factor for the recent rapid spatial growth of the city. Other factors include the establishment of institutions of higher learning, namely, Hassan Usman Polytechnic, a Federal college of Education and recently two Universities (Katsina Islamic university and Umar Musa Yar'adua University). As a result, farmland, Plantations and open spaces around and within the city are gradually being converted into built-up environment containing buildings and other related physical structures such as roads.

Urbanization is defined as the development of cities and suburban areas due to population growth leading to major changes in land use/land cover in accordance with human activities. Population growth in urban areas results in the use of more impervious land in the construction activities (Doygun & Ilter, 2007, Deniz, Esbah, Kucukerbas & Sirin, 2008) cited in (Kaya *et al*. 2012). Globally, land cover today is altered principally by direct human use: agriculture and livestock raising, forest harvesting and management, and urban and suburban construction and development. Hardly can we find any vegetation that has not been affected by man in the world. About 400,000 hectares of vegetation cover has been confirmed to be lost annually (Adesina, Siyanbola, Okelola, Pelemo, Ojo & Adegbulugbe, 1999) cited in (Balogun, Adeyewa, Balogun & Morakinyo, 2011). Due to anthropogenic activities, the earth surface is being significantly altered in some manner and man's presence on earth and his use of land has had a profound effect on rather all meteorological/climate parameters. Land transformation has been asserted to be one of the most important fields of human induced environmental transformation (Fasal, 2000) cited in (Balogun *et al*, 2011).

A most noticeable phenomenon that has arisen as a result of city expansion is that urban climates are warmer and more polluted than their rural counterparts. This is because the low values of albedo, vegetative cover, and moisture availability in combination with the presence of high levels of anthropogenic heating have given rise to a phenomenon known as the urban heat island (UHI)

effect. Hence, urban areas generally act as islands of elevated temperature relative to the natural areas surrounding them (Sailor, 1995) cited in (Lo & Quattrochi, 2003). The main cause of the Urban Heat Island is the modification of the land surface through urban development with the use of materials that effectively retain heat. As population increase, they tend to modify a greater area of land and have a corresponding increase in the average temperature (Rail, 2007). Urbanization, on the other hand, negatively affects the environment due to pollution modifying the physical and chemical properties of the atmosphere and the soil surface. UHI is considered to be a cumulative effect of all these impacts. It is defined as the rise in temperature of any man-made area (Kaya *et al*., 2012).

The integration of remote sensing and geographic information systems (GIS) has been widely applied and recognized as a powerful and effective tool in detecting urban land use and land cover change (Ehlers, Jadkowski, Howard and Brostuen, 1990; Treitz, Howard and Gong, 1992; Harris and Ventura, 1995) cited in Saleh (2010). Satellite remote sensing collects multispectral, multi resolution and multi temporal data, and turns them into information valuable for understanding and monitoring urban land processes and for building urban land cover datasets. GIS technology provides a flexible environment for entering, analyzing and displaying digital data from various sources necessary for urban feature identification, change detection and database development (Weng, 2001).

1.2 STATEMENT OF THE RESEARCH PROBLEM

It is a well known and documented fact that urbanization can have significant effects on local weather and climate. One of the most familiar effects of urbanization is the urban heat island, which is the direct representation of environmental degradation. An urban heat island is a metropolitan area which is significantly warmer than its surrounding rural areas. The interactions of urban surfaces with the atmosphere are governed by surface heat fluxes, the distribution of

which is drastically modified by urbanization. Urbanization has changed city environment greatly, owing to the replacement of vegetation by asphalt and concrete and increase in population and anthropogenic heat (Zhang & He, 2006). Consequently, estimating surface temperature (ST) is a key step to the analysis of urban heat island.

The analysis of temporal remote sensing data helps in understanding land use/land cover changes and their impact on the environment. The thermal infrared bands of remote sensing data of space borne sensors help to retrieve ST. ST is the measure of heat emission from land surface due to various activities associated with the land surface. In addition to ST measurements, these thermal infrared (TIR) sensors may also be utilized to obtain emissivity data of different surfaces with varied resolutions and accuracies. Surface temperature and emissivity data are used in urban climate and environmental studies, mainly for analyzing ST patterns and its relationship with surface characteristics, for assessing surface urban heat island, and for relating land surface temperature with surface energy fluxes in order to characterize landscape properties, patterns, and processes (Quattrochi & Luvall, 1999).

Studies on the Urban Heat Island (UHI) phenomenon using satellite remote sensing data have been conducted by many researchers. The first surface urban heat island (SUHI) observations (from satellite based sensors) were reported by Rao (1972), demonstrating that urban areas could be identified from the analyses of thermal infrared data acquired by a satellite. Falahatkar, Hosseini and Soffianian (2011) study of the relationship between land cover changes and spatial-temporal dynamics of land surface temperature evaluated the land cover change detection in Isfahan and analyzed the impact of these changes on surface temperature using thematic mapper (TM) and enhanced thematic mapper plus (ETM+) thermal bands for 1990 and 2001. The results indicated that bare land exhibits the highest surface radiant temperature (44.9°C in 1990 and 48.9°C in 2001), followed by stony body (42.6°C in 1990 and 45.3°C in 2001).

Many researchers have employed remote sensing and GIS to study the relationship between land surface temperature and land use/land cover, NDVI, population, etc. For instance, Weng (2001) reported an investigation into the application of the integration of remote sensing and geographic information systems (GIS) for detecting urban growth and assessing its impact on surface temperature. The results revealed a notable and uneven urban growth in the study area. In Jimeta, Adamawa state Nigeria, Zemba, Adebayo and Musa (2010) reported the application of the integration of remote sensing and geographic information systems (GIS) for detection of urban growth and assessing its impact on surface temperature. The results also revealed a notable and uneven urban growth in the study area. Urban development had raised surface radiant temperature by 9^{o}C from 1986 to 2008 in the urbanized area. Tyubee and Anyadike (2013) also used remote sensing in conjunction with Geographic Information System (GIS) to determine the relationships between land use/land cover (LULC) and surface temperature, and surface temperature and atmospheric temperature (AT) in Makurdi, North central Nigeria. The study concludes that both vegetation cover and moisture diminish ST but the cooling potential of the latter is higher than the former. Built-up structures enhance ST, which in turn enhances AT particularly during daytime.

Many studies outside Nigeria have employed remote sensing and GIS to estimate the effect of urban heat island, but most of the works embarked upon in Nigeria, especially in the north-western part of Nigeria, used land based observation and in-situ field measurements of air temperature and only a few adopted remote sensing and GIS approach. Abdulhameed, Iguisi, Ati, Sawa and Nduka (2012) collected and analyzed Canyon geometry data sky view factor (SVF) and temperature data from the sites to study the Characteristics of urban canopy heat island in Kano metropolis. The UCHI characteristics indicated that the highest UCHI intensity was observed during the daytime period while lower intensities were observed during the night time periods. The

results also revealed that the April study period has the highest intensities, followed by the August, then the January period.

In Katsina metropolis, the only documented research on urban climate was done by Gide (2012) in which he investigated the impact of urban growth on the microclimate in the city. He examined the microclimate of Katsina metropolis and a nearby rural control station for forty years; assessing the difference between the microclimate of the town and the nearby rural control site. He also examined the trends in population of the town and assessed the relationship between the microclimate of the metropolis and population growth of the town. The result showed that urban growth has impact on the microclimate of Katsina metropolis. Gide (2012) did not use remote sensing and GIS techniques to categorize and analyze the land use/land cover types, and estimate the surface temperature of the various land use/land cover types in the study area. This is the research gap that needs to be bridged.

This research employed remote sensing and GIS in assessing environmental changes, and of the rate of urban growth in Katsina metropolis and to analyze the effects of such growth on surface temperature. The application of remote sensing and GIS will bring an improvement in the generation, integration and presentation of precise data on the elements of climate in urban centres and their surrounding areas and will address the limitations of the in situ approach in the quantitative description of areal extent and help in ascertaining the exact spatial variation in the distribution of micro climates on both local and global scales. To be able to do this effectively, the following question will be answered:

i. What are the various classes of land use and land cover in Katsina metropolis within the study period (1986, 1999 and 2014)?
ii. What is the rate of land use/land cover change in the study area?
iii. What is the magnitude of surface temperature in Katsina metropolitan area?

iv. What is the average surface temperature value of each land use land cover type?

1.3 AIM AND OBJECTIVES OF THE STUDY

The aim of this research was to evaluate the effects of urban growth on temporal variations of surface temperature in Katsina metropolis. This was achieved through the following objectives, to:

i. map out the various land use/land cover types of Katsina metropolis within the study period (1986, 1999 and 2014).
ii. evaluate the land use/land cover changes within the study period.
iii. compute the Surface temperature of the study area from Landsat TM (1986), Landsat ETM (1999) and Landsat8 TIRS (2014) data.
iv. estimate the average surface temperature value of each land use land cover type in Katsina metropolis.

1.4 SCOPE OF THE STUDY

The study covers Katsina metropolis which comprises Katsina and part of Batagarawa, Kaita and Jibia Local Government Areas in Katsina state, northern Nigeria. The effects of urban growth on temporal variations of surface temperature in Katsina metropolis using only remote sensing and GIS approach was carried out for a period between 1986 and 2014 using Landsat TM (1986), ETM+ (1999) and Landsat 8 (2014). Specifically, the study investigated changes in land use and land cover, as a result of urban expansion over time and how this relates to urban surface temperature.

1.5 JUSTIFICATION OF THE STUDY

Ecosystems in the northern part of Nigeria are vulnerable to climate change. Reliable temperature data are indispensable for assessing the region's response to global warming. Unfortunately, air temperature data for northern areas are lacking or of poor quality due to the small number of weather stations which are usually located in airports. Surface temperature derived from satellite

images may complement or substitute for air temperature data. The research will provide information about surface temperature from satellite images of Katsina metropolis, which could serve as a primary resource for further environmental and climatology studies.

Due to rapid urban growth that have been taking place in Katsina metropolis over the years and the possible effects on the microclimate in the area, it is believed that, urban problems being neglected will increase with time and space. Many people in the developing countries like Nigeria don't know how urban growth influences microclimate of cities, let alone ways of handling the situation. It is, therefore, important to analyze the effects of urban growth on Surface temperature in Katsina metropolitan area in order to create awareness about the ever worsening effect of urban heat island and recommend mitigating strategies.

The energy implications of the climatic changes induced by UHI have received very little attention in urban design and planning. There is an important relationship between land use/land cover changes and UHI intensity (Chen, Zhao, Li, & Yin, 2006, Baek, Kim, Lim & Lee, 2011). Defining this relationship is of utmost significance regarding land use/land cover planning. The findings of this study can be used by urban planning and policy makers to for example, introduce zoning by-laws or building codes that require new industrial or commercial development to include green spaces and green or high-albedo roofing.

CHAPTER TWO: CONCEPTUAL FRAMEWORK AND LITERATURE REVIEW

2.1 INTRODUTION

In this chapter, some theoretical principles involved in urbanization, urban climate and urban heat island were reviewed. Previous studies on the effects of urban growth on surface temperature, the causes and effects of UHI at local and regional scales were also reviewed along with. Finally, the adaptation measures to help organizations and individuals cope with UHI effects were discussed

2.2 CONCEPTUAL FRAMEWORK

2.2.1 Concept of Urbanization

The definition of 'urban' varies from country to country, and, with periodic reclassification, can also vary within one country over time, making direct comparisons difficult. An urban area can be defined by one or more of the following: administrative criteria or political boundaries (e.g., area within the jurisdiction of a municipality or town committee), a threshold population size (where the minimum for an urban settlement is typically in the region of 2,000 people, although this varies globally between 200 and 50,000), population density, economic function (e.g., where a significant majority of the population is not primarily engaged in agriculture, or where there is surplus employment) or the presence of urban characteristics (e.g., paved streets, electric lighting, sewerage) (UN-Habitat, 2012).

The (relative or absolute) increase in the number of people who live in towns and cities. The pace of urban population growth depends on the natural increase of the urban population and the population gained by urban areas through both net rural-urban migration and the reclassification of rural settlements into cities and towns (UN-Habitat, 2012). In this study urban growth will be looked at in the context of spatial growth.

2.2.2 Concept of Urban Heat Island

The urban heat island effect (UHI) is the temperature difference between urban and surrounding rural areas. This phenomenon occurs due to the patterns of urban development which result in the conversion of vegetated, permeable land areas into urban landscapes dominated by high albedo (i.e. measure of the amount of solar energy that is reflected by a given surface) and impervious surfaces that absorb a high percentage of solar radiation (Rosenzweig, Solecki & Slosberg, 2006). Typically the temperature difference between urban and rural areas ranges from 3-5°C during the day. However, at night the difference can reach as high as 12°C due to the slow radiation of heat from urban surfaces (Environmental Protection Agency, 2008).

While the UHI occurs year-round, the magnitude of its effect is variable, in large part due to changes in meteorological conditions (Solecki, Rosenzweig, Pope, Parshall & Wiencke, 2003). The effect is most intense on calm, clear days in the summer and fall. This is because on clear days, short-wave radiation from the sun travels on a direct path to the earth's surface, and is not obstructed by clouds which can reflect a large proportion of incoming solar radiation (Rosenzweig, Solecki & Slosberg, 2006). There are two types of UHIs namely 1) atmospheric urban heat island and 2) surface urban heat island.

2.2.2.1 Atmospheric urban heat islands

Atmospheric urban heat islands can be divided into two different categories: 1) Canopy Layer Heat Island (CLHI) and 2) Boundary Layer Heat Island (BLHI). The CLHI refers to the layer of air closest to the surface which extends to approximately building height. The BLHI is located above the canopy layer and may be up to 1 kilometre or more in thickness by day and a few hundred meters in thickness at night (Voogt, 2004).

2.2.2.2 Surface urban heat island

The Surface Urban Heat Island (SUHI) refers to the relative warmth of urban surfaces compared to surrounding non-urbanized surfaces. While the atmospheric UHI can be detected by ground-based air temperature measurements, the SUHI is typically characterized as a measurement of Land Surface Temperature (LST), based on the use of thermal remote sensing (Rose & Devadas, 2009). SUHIs are generally strongest during the day but are usually present during the night as well. Similar to UHIs, the magnitude of SUHIs is influenced by sun intensity, LULC characteristics and vegetation abundance. SUHIs are typically largest during the summer and their intensity tends to vary much more than that of UHIs (EPA, 2009). The difference in daytime surface temperatures between urban and rural areas is on average 10 to 15°C, however, at night the difference in surface temperatures between the two tends to average only about 5 to 10°C (Voogt & Oke, 2003).

2.2.3 Relationship between Surface and Air Temperatures

LSTs are considered to be a reliable indicator of the UHI as there is generally a high correlation between LSTs and air temperatures in the canopy layer, due to the transfer of thermal energy emitted from the surface to the atmosphere (Nichol, 1994; Arrau & Pena, 2010). However, due to the fact that air mixes within the atmosphere, the relationship between surface and near-surface air temperatures is not constant (Environmental Protection Agency, 2009). As can be observed in Figure 2.1, atmospheric temperatures normally fluctuate less than surface temperatures across a given area during the day, while a more congruent relationship between atmospheric and surface temperatures can be observed during the nighttime hours.

2.2.4 Urban Heat Island Intensity

UHI's are usually most pronounced during the nighttime as the majority of urban materials tend to absorb heat during the day which is then only slowly released during the nighttime hours (see Fig 2.1). This is due to their high thermal inertia. By the time most rural surfaces have already experienced cooling after sunset; most urban materials will have only partially cooled, releasing heat at a much slower rate (Arrau & Pena, 2010). The result is a modified urban climate, much warmer than its non-urbanized surroundings (Rose & Devadas, 2009). Moreover, the differential cooling rates between urban areas and their rural peripheries are usually most distinct on calm and clear nights. It has been found that cities with populations of 1 million or more average 1 to 3°C warmer in atmospheric temperature as compared to their rural surroundings (Environmental Protection Agency, 2009). However, in some cases this temperature discrepancy has been measured to be as much as a 12°C difference (University of Manchester, 2007).

The magnitude of an UHI is known as UHI intensity, which can be defined as the air temperature difference between urban and rural areas. UHI intensity is influenced by climate region, local topography, industrial development of a city (Stathopoulou, Cartalis & Petrakis, 2005) city size and density, Land-Use/Land-Cover (LULC) characteristics, the characteristics of the surrounding rural areas (Fortuniak, 2009) and vegetation abundance (Santana, 2007). Meteorological conditions (especially wind speed and cloud cover) and sun intensity also influence the development of the UHI – and therefore, UHI intensity tends to vary both hourly and seasonally (EPA, 2009). Of all the factors mentioned above, LULC characteristics and the abundance of urban vegetation are the two factors which are considered to have the most significant effect on UHI intensity, as well as on intra-urban thermal patterns (Xian & Crane, 2006; Arrau & Pena, 2010).

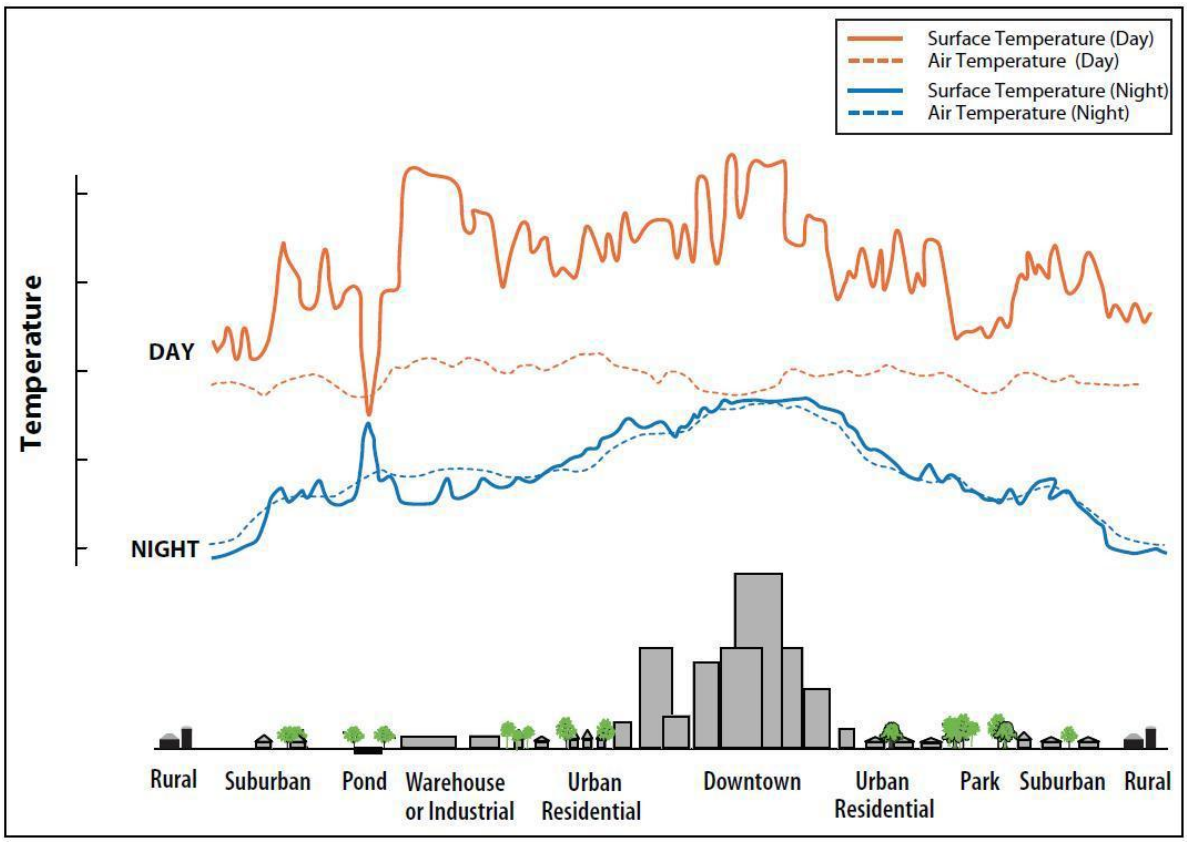


Figure 2.1: Differences between surface and air temperature during the day and at night

.

Source: Urban Heat Island Basics, 2008.

2.2.5 Urban surface energy balance

The modification of the Earth's surface due to processes of urbanization, e.g. the increased urban surface area, the use of impervious and high heat capacity materials, the reduction of vapotranspiration, the increased runoff and so on, significantly alters the surface energy balance and the dynamic and thermodynamic nature of the boundary layer. Combined with anthropogenic heat emission and pollutants, all of these processes lead to distinct urban climates (Oke, 1987; Grimmond, 2007) Cited in (Yang, 2013).

The energy balance of the surface is the physical process that determines the surface fluxes of temperature and moisture. Energy conservation can be expressed as,

$S^{+} + S^{-} + L^{+} \square L^{-} \square H \square G \square LE = 0$

S^+ and S^- are the incoming and outgoing shortwave radiation respectively. L^+ and L^- are the downward and upward long wave radiation respectively. H is the sensible heat flux into the boundary layer, G is the conductive heat flux into the urban fabric, and LE is the latent heat due to the evaporation of water (Yang, 2013).

The energy budget of artificial surfaces, such as asphalt and concrete, is quite different from that of natural surfaces due to the different thermal and radiation properties. Anandakumar (1999) studied the energy budget components of a dry asphalt surface by observation. Throughout the year, the ground conductive heat flux G is found to be of larger magnitude than that of the sensible heat flux H. During the cool season, most of the net radiation is transformed into G, while in the warm season, a great amount of heat is transferred into H as the incoming energy is higher. Similar findings are verified by other studies, which reveal that the artificial materials cause very large sensible heat fluxes during a typical summer day, which often continue positive although are smaller after sunset, especially for asphalt, which releases the largest amount of H compared with various other pavement surfaces (Kotani & Sugita, 2005; Herb et al., 2008; Takebayashi & Moriyama, 2012). In contrast, H is greatly reduced in grassy areas or bare soil surfaces due to evapotranspiration, especially during the growing season when almost all the incoming heat is partitioned into G and LE (Kotani & Sugita, 2005; Takebayashi & Moriyama, 2012). Also, both the high-albedo material surfaces and grassy surfaces are able to dramatically reduce the peak and daily total energy received by increasing the S^-, as well as by the shading effect and increasing the latent heat flux LE, respectively, and provide further benefits to the indoor environment in summer if such material is used for building fabric (DelBarrio, 1998; Sailor, 2008; Meyn & Oke, 2009; Scherba et al., 2011) cited in (Yang, 2013).

2.3 LITERATURE REVIEW

2.3.1 Urban Growth in Nigeria

Ayedun, Durodola and Akinjare (2011) reported that the advent of petroleum in the Nigerian economy in the late 60s and early 70s brought with it advantages. The main advantages were increase in government revenue, noticeable rise in industrial investment both in the public and private sectors, balance of payment surplus, growth in construction industries, rapid urbanization and ostensible advancement in educational, health and infrastructural development. In fact, by the time the Third National Development Programme was launched in 1973, it was said that money was no longer a problem in the economic development of Nigeria but how to manage it.

The era of numerous creation of states and local governments in Nigeria has resulted into unprecedented acceleration of urbanization processes in all state capitals nation-wide to the extent that it is feared that city dwellers in the country have outnumbered those residing in the rural areas and yet many more people are still desirous of moving into cities in search of paid employment (Ayedun, Durodola & Akinjare, 2011).

The last fifty years of the 20th century witnessed unprecedented urbanization in Nigeria. For example, in 1890, there were 25 urban centres in the country. This figure increased by 125 percent (i.e. 56) in 1953. Between 1953 and 1963 the number again grew from 56 urban centres to 185 which represent about 229 percent increase over only a period of ten years. While the total urban population increased by about 240 percent between 1890 and 1953, the population increased by more than 300 percent between the period of 1953 and 1993. In fact a reliable estimate put urban population in the country at present at more than 35 percent of the entire country's population. The figure is expected to reach about 62 percent by the year 2025. The implication of this is that, within a period of less than 15 years from now, a population which is larger than half of the

present total population of Nigeria will constitute the new arrivals to the urban scene in Nigeria, if all other factors relating to these trends continue unchecked (Ayedun, Durodola & Akinjare, 2011).

2.3.2 Spatial Growth of Katsina Metropolis

Katsina city like most urban centers in sub Sahara African is experiencing high rates of urbanization due to the increasing population densities (consequent of the natural population increase and migration) and the inevitable natural phenomenon of spatial growth with resultant rampant changes in the use of land and buildings. The urbanization process of Katsina provides a unique character of a rural-urban transformation ignited by a political transformation that combined both socio-economic and spatial growth in a rapid manner. As a result, the un-built land in/ around is gradually being converted into built-up environment containing buildings and other related physical structures such as roads.

Adulkadir (2009) used geomatics technology to analyze the pattern of spatial growth in Katsina metropolis and discovered that between 1977 and 2007, the size of the urban area had increased by 3381.34ha. This is a clear indication that the city is expanding at a rapid rate.

2.3.3 Causes of Urban Growth

2.3.3.1 Population growth

There are three components of urban population growth: natural growth of urban population, rural-urban migration and the reclassification of areas previously defined as rural. Natural increase provides a base for urban population growth rates, and rural-urban migration and reclassification supplement this growth. Anyhow the natural increase of the population in the city often declines sharply together with the urbanization process, that has happened for example, in Thailand, Malaysia and Indonesia (Stutz & Souza, 1998).

2.3.3.2 Economic growth

Expansion of economic base (such as higher per capita income, increase in number of working persons) creates demand for new housing or more housing space for individuals (Boyce, 1963; Giuliano, 1989; Bhatta 2009). This also encourages many developers for rapid construction of new houses. Rapid development of housing and other urban infrastructure often produces a variety of discontinuous uncorrelated developments. Rapid development is also blamed owing to its lack of time for proper planning and coordination among developers, governments and proponents.

2.3.3.3 Standard of living

The differences in standard of living are major issues when considering factors that encourage urbanization. Higher living standards and higher salaries in the city attract people to move to the cities. As long as the income gap between rural and urban areas is big, people tend to move to the cities. Economic factors and employment are the main reasons for migration. Sometimes the employment in rural areas is non-existing. In these cases moving to the city, even for very low salaries, is more profitable than staying in the countryside (Sajor, 2001; Brookfield & Byron, 1993). Political and social factors are also better in the urban areas and they are one reason for migration. In the city health care and social relations are much easier to organize which makes the inhabitants feeling more secure. In the city people may more easily have they voices heard by joining different political groups and by this poor people can require better living standards and services (Bhatta, 2010).

2.3.3.4 Environmental pressure

The biggest environmental pressure for rural people is the lack of profitable land. The land inherited from the parents is divided to the children and their children. At last the land per farmer becomes so small that it is unprofitable to farm. On the other hand erosion and land deterioration

makes farming even more difficult. Even when poor farmers have enough land space they can't always afford and compete for non-sufficient water resources or fertilizers. Water is sometimes much polluted and regulations forbid the use of that kind of water because of food contamination. This gives no opportunity to the poor farmers. They can either continue farming with contaminated water and get caught with the contamination of crops or try to find some other livelihood. This is the problem in lower basins of many rivers in developing countries (Sajor, 2001).

Water shortage increases social inequity. Poor farmers cannot sink boreholes to the necessary depths to extract water. Wealthier farmers can benefit by moving inland to buy up more land or water. The only way to survive for these poor farmers is to move to cities to find some non-agricultural livelihood (UNEP, 1999).

2.3.3.5 Transportation

Transportation routes open the access of city to the countryside and responsible for linear branch development. The construction of expressways and highways cause both congestion in the city and rapid outgrowth (Harvey & Clark, 1965). Important to realise that transportation facilities are essential to cities and its neighbourhoods. Development of urban economy and thereby job opportunities are directly dependent on the transportation facilities. Therefore, transportation facilities can never be suppressed; rather initiatives to impede linear branch development by means of government policies and regulations should be practiced.

2.3.3.6 Industrialisation

Establishment of new industries in countryside increases impervious surfaces rapidly. Industry requires providing housing facilities to its workers in a large area that generally becomes larger than the industry itself. The transition process from agricultural to industrial employment demands more urban housing. Single-storey, low-density industrial parks surrounded by large

parking lots are one of the main reasons of sprawl. There is no reason why light industrial and commercial land-uses cannot grow up instead of out, by adding more storeys instead of more hectares. Perhaps, industrial sprawl has happened because land at the urban edge is cheaper (Bhatta, 2010).

2.3.4 Consequences of Rapid Rate of Urban Growth

2.3.4.1 Loss of farmland

Urban growth, only in the United States, is predicted to consume 7 million acres of farmland, 7 million acres of environmentally sensitive land, and 5 million acres of other lands during the period 2000–2025 (Burchell, Downs, McCann & Mukherji, 2005). This case is enough to visualise the world scenario.

Provincial tax and land-use policies combine to create financial pressures that propel farmers to sell land to speculators. Low prices of farm commodity in global markets often mean it is far more profitable in the long term for farmers to sell their land than to continue farming it. In addition, thousands of relatively small parcels of farmland are being severed off to create rural residential development. Collectively, these small lots contribute to the loss of hundreds of hectares of productive agricultural land per year.

.The loss of agricultural land to urban sprawl means not only the loss of fresh local food sources but also the loss of habitat and species diversity, since farms include plant and animal habitat in woodlots and hedgerows. The presence of farms on the rural landscape provides benefits such as greenspace, rural economic stability, and preservation of the traditional rural lifestyle.

2.3.4.2 Increase in temperature

According to Bhatta (2010) increase in temperature in urban areas is caused by two factors. First, dark surfaces such as roadways and rooftops efficiently absorb heat from sunlight and reradiate it

as thermal infrared radiation; these surfaces can reach temperatures of 50–70◦ F (28–39◦ C) higher than surrounding air. Second, urban areas are relatively devoid of vegetation, especially trees; that would provide shade and cool the air through evapotranspiration. As cities grow, the heat island effect expands both in geographic extent and in intensity. This is especially true if the pattern of development features extensive tree-cutting and road construction (Bhatta, 2010).

Furthermore, dispersed metropolitan expansion involves a positive feedback loop that may aggravate the heat island effect. Greater travel distances, generate a large amount of automobile travel and this in turn, results in more fuel combustion, with more production of carbon dioxide, and consequent contributions to global climate change. Global climate change, in turn, may intensify the heat island effect in metropolitan areas. Thus, not only does the morphology of metropolitan areas contribute to warming, but so may the greenhouse gas production that results from increased driving (Bhatta, 2010).

2.3.4.3 Poor air quality

Urban growth contributes to poorer air quality by encouraging more automobile use, thereby adding more air pollutants such as carbon monoxide, carbon dioxide, ground-level ozone, sulphur dioxide, nitrogen oxides, volatile organic carbons, and microscopic particles (Frumkin, 2002). These pollutants can inhibit plant growth, create smog and acid rain, contribute to global warming, and cause serious human health problems.

Increased temperature in urban areas also has indirect effects on air pollution. As the temperature rises, so does the demand for energy to power fans, air coolers, water coolers, and air conditioners; requiring power plants to increase their output. The majority of power plants burn fossil fuels, so increased demand of power in summer results in higher emissions of the pollutants they generate, including carbon dioxide, particulate matter, sulphur oxides, nitrogen oxides, and

air toxics. Furthermore, ozone formation from its precursors, nitrogen oxides and hydrocarbons, is enhanced by heat (Frumkin, 2002).

2.3.4.4 Effects on water quality and quantity

Urban growth and lead to an increasing imperviousness, which in turn induces more total runoff volume. So urban areas located in flood-prone areas are exposed to increased flood hazard, including inundation and erosion (Jacquin, Misakova & Gay, 2008). As new development continues in the periphery of the existing urban landscape, the public, the government, planners and insurance companies are more and more concerned by flooding disasters and increasing damages (Wisner, Blaikie, Cannon & Davies, 2004; Jacquin, Misakova & Gay, 2008).

In the urban area, water runs off into storm sewers and ultimately into rivers and lakes. Extra water during heavy rain can dramatically increase the rate of flow through wetlands and rivers, stripping vegetation and destroying habitats along riverbanks. It can also cause damaging floods downstream and lead to an increase in water pollution from runoff contaminated with lawn and garden chemicals, motor oil and road salt. Widely dispersed development requires more pavements that cause more urban runoff that pollutes waterways (Lassila 1999; Wasserman 2000). These pollutants can be absorbed by humans when they eat contaminated fish from affected water-bodies and when they drink from contaminated surface water or groundwater sources.

2.3.5 Thermal Remote Sensing of Urban Surface Temperature

In urban areas, natural vegetation is often removed and replaced by non-evaporating, non-transpiring impervious surfaces. Under such alteration, the partitioning of incoming solar radiation into fluxes of sensible and latent heat is skewed in favour of increased sensible heat flux as evapotranspirative surfaces are reduced. A higher level of latent heat exchange is found with more

vegetated areas, while sensible heat exchange is more favoured by sparsely vegetated urban areas that have large amounts of impervious surfaces (Oke, 1982). The land surface temperature (LST) pattern is a manifestation of existing surface energy balance and has been extensively studied with thermal remote sensing technology.

Satellite thermal infrared sensors measure top of the atmosphere (TOA) radiances from which brightness temperatures of land surfaces (also known as blackbody temperatures) can be derived using Plank's law (Dash, Göttsche, Olesen & Fischer, 2002). The difference between the TOA and land surface brightness temperatures ranges generally from 1 K to 5 K in the 10 to 12 _m spectral region, subject to the influence of the atmospheric conditions (Prata *et al*., 1995). Research on LST shows that the partitioning of heat fluxes and thus surface energy response is a function of varying surface soil water content and vegetation cover (Owen, Carlson & Gillies, 1998). For nonvegetated areas, LST measurements typically represent the radiometric temperatures of sunlit surfaces, such as bare soil and impervious surface. As the amount of vegetation cover increases, the radiative temperature recorded by a sensor approximates more closely the temperatures of green leaves and the canopy temperature at spectral vegetation maximum or complete canopy cover (Goward *et al*., 2002). The observed portion of vegetation and non-vegetation surfaces can vary with the viewing angle, thus the amount of vegetation (ground) alters as the observation angle increases (Caselles *et al*., 1992).

Generally speaking, LST are a function of four surface and subsurface properties: albedo, emissivity, thermal properties of urban construction materials, and the composition and structure of urban canopy (Goward, Xue & Czajkowski, 1981). Moisture is included in the thermal properties of materials. Each of these characteristics displays a wide range of variation in urban contexts. Following discussion focuses on the relationship between LST and the three urban landscape components identified in the Ridd model: vegetation, impervious surface, and soil.

Impervious surfaces refer to two major functional categories of urban surfaces: rooftops and the transportation system (roads, parking lots, driveways, and sidewalks) (Schueler, 1994). Impervious surfaces trigger local decreases in infiltration, percolation and soil moisture, reductions in natural interception and depression storage and increases in runoff (Brun & Band, 2000). As a result, impervious surfaces in the urban context experience an almost dichotomous wet/dry behaviour, affecting local partitioning of daytime radiant energy (Oke, 1982). The surface energy balance of impervious surfaces is characterized by partitioning of the net radiance into sensible heat and heat conducted to the substrate (i.e., storage heat flux) (Oke, 1982). The energy balance systems may vary considerably with site geometries and construction materials. The influence of geometry may vary with the changes in building density, height, and size, and street canyon orientation. High-rise buildings are found to be cooler than low-rise buildings and non-built areas because the latter have a greater portion of active horizontal surface and low buildings cast shorter shadows, while smaller buildings with smaller building mass tend to have lower thermal inertia, leading to a quicker heat accumulation during the daytime (Nichol, 1996).

For any surface material, certain internal properties, such as heat capacity, thermal conductivity and inertia, play important roles in governing the temperature of a body at equilibrium with its surroundings (Campbell, 2002). Dry, bare, and low-density soils, for example, are linked to high LST owing to relatively low thermal inertia (Carnahan & Larson, 1990). The emissivity of soils is a function of soil moisture conditions, and soil density (Larson & Carnahan, 1997).

Surface temperature is the main thing that is important to the study of the urban climate, not only in obtaining boundary conditions of the atmosphere, but also in understanding the environmental conditions necessary for human population (Hung & Uchihama, 2006). Thermal infrared (TIR) bands of a satellite sensor are able to detect surface temperature distributions. Satellite imagery

has been used for the study of UHI to analyze and determine how and why certain city areas contribute to heat island (Nichol, 1996; Unger, Sumeghy & Zoboki, 2001; Weng, 2009).

2.3.6 Application of Remote Sensing and GIS in Urban Temperature Studies

The integration of remote sensing and geographic information systems (GIS) has been widely applied and been recognized as a powerful and effective tool in detecting urban land use and land cover change (Ehlers, Jadkowski, Howard, & Brostuen, 1990, Treitz, Howard & Gong, 1992, Harris & Ventura 1995). Satellite remote sensing collects multispectral, multiresolution and multitemporal data, and turns them into information valuable for understanding and monitoring urban land processes and for building urban land cover datasets. GIS technology provides a flexible environment for entering, analyzing and displaying digital data from various sources necessary for urban feature identification, change detection and database development.

Many researchers have employed remote sensing and GIS to study the relationship between land surface temperature and land use/land cover, NDVI, etc. For instance, Srivanit and Hokao (2012) studied the impact of urbanisation on the thermal environment of Bangkok Metropolitan Area. They used normalized difference vegetation index to extract land use/land cover information from remote sensing images of different time periods and then analyzed the surface temperature retrieved from the thermal infrared band. The results indicated that urban/built-up areas expanded dramatically, while agricultural land declined. Moreover, temperature differences between the urban/built-up and the surrounding rural areas significantly widened.

In Japan Laosuwan and Sangpradit, (2012), evaluated the effect of urban heat island by using land sat-5 thematic mapper data and knowledge based method. They investigated the urban heat island (UHI) effect by analyzing Normalized Difference Vegetation Index (NDVI) and Normalized Difference Build-up Index (NDBI). Saleh (2010) reported an investigation into the application of the integration of remote sensing and geographic information systems (GIS) for detecting urban built

up growth for the period 1961-2002, and evaluated its impact on surface temperature in Baghdad city . The purpose of this study was to analyze and verify the spatial distribution property of the surface temperature with urban spatial information that are related with land cover / land use and NDVI using remotely sensed data and GIS.

Many researchers have employed remote sensing and GIS to study the relationship between land surface temperature and land use/land cover, NDVI, population, etc.

2.3.7 Causes of Urban Heat Island

In addition to the local climate, which is influenced by various meteorological parameters such as temperature, relative humidity and wind, a number of anthropogenic causes promote the emergence and intensification of urban heat islands. These causes are greenhouse gas emissions, gradual loss of urban forest cover, the impermeability and low albedo of materials, the thermal properties of materials, urban morphology and the size of cities as well as anthropogenic heat.

2.3.7.1 Vegetation removal

One of the key factors that contribute to the UHI is the loss of permeable, vegetated landscapes. Vegetation and trees cool landscapes through the shading they provide as well as through evapotranspiration. Shading is primarily provided by larger vegetation such as trees and helps prevent solar radiation from being absorbed by areas and features below the canopy. The solar radiation reaching the canopy may be used for plant processes such as photosynthesis, while some solar radiation is reflected into the atmosphere. As a result, measurable differences can be found in the temperature of surfaces below the tree canopy compared to unshaded surfaces (Environmental Protection Agency, 2008). Therefore, as trees and vegetation are removed, the proportion of solar radiation that is reflected decreases, resulting in warming.

The presence of vegetated landscapes also facilitates cooling through evapotranspiration. Evapotranspiration occurs as plants absorb liquid water and release it into the atmosphere as water vapour. During this process, energy from solar radiation is used and transformed by plants into latent heat rather than sensible heat, which cools the ambient air surrounding vegetation (Bowler, Buyung-Ali, Knight & Pullin, 2010). As vegetation is lost, soil moisture content and evapotranspiration rates decrease, resulting in air temperature increases that cause the UHI. Measurable differences in evapotranspiration rates have been identified in academic studies. For instance, it was determined that evapotranspiration decreased by 38% in Tokyo from 1972 to 1995 due to urbanization (Rizwan, Dennis & Chunho, 2008).

2.3.7.2 Properties of urban materials

According to DeCarolis (2012) as vegetation is lost, the conversion of landscapes into areas dominated by urban infrastructure and impermeable surfaces occurs. She said urban areas are primarily made up of pavement and roofing surfaces and the surfaces are constructed with materials that cause the UHI by altering how solar radiation is reflected, emitted, and absorbed.

One of the key properties that impacts the absorption and reflection of solar radiation is albedo. Albedo is a measure of the amount of solar energy that is reflected by a given surface, expressed as a value between 0 (total absorption) and 1 (total reflectance). As a general rule, white and light coloured materials have a high albedo, while darker materials have low albedo (Forkes, 2010). The various albedos of common In addition to albedo, emissivity, a measure of the amount of heat a surface radiates per unit area at a given temperature, also has an important role in causing the UHI. Surfaces with low emissivity release heat slowly, causing areas to retain heat and warm air temperatures (Environmental Protection Agency, 2008).

Commonly used paving materials such as asphalt and cement typically have albedos ranging from 0.05-0.4, and high emissivity values of approximately 0.8-0.9. These high emissivity values are

similar for roofing materials with the exception of metal roofing, which has very low emissivity at approximately 0.05-0.3 (Houston Advanced Research Center, 2009). Advances in the development of new pavement and roofing materials will help reduce the UHI by reflecting increasing amounts of solar radiation (DeCarolis, 2012).

It is also important to note that the thermal properties of urban materials may change over time. With respect to asphalt pavement, its albedo tends to improve over time due to weathering. Conversely, the albedo of cement generally declines with age due to the accumulation of dirt and debris on the originally light surface. A similar process occurs on roofing materials, as the collection of dirt and debris results in their albedo decreasing over time. As a result, it is important for planners to recognize these potential changes when selecting urban materials in order to accurately assess their potential impact on the UHI (DeCarolis, 2012).

2.3.7.3 Urban geometry

In addition to the properties of infrastructure and surfaces in urban areas, the geometry of urban structures can influence the UHI by changing patterns of absorption and reflectance of solar radiation (DeCarolis, 2012). The arrangement of buildings can increase the absorption of incoming solar radiation in cities. Without the presence of multiple buildings, solar radiation would typically be absorbed and reflected into the atmosphere by only one surface. However, buildings may interfere with this process by absorbing and reflecting radiation multiple times and by more than one surface. This results in an increase in the total amount of radiation that is absorbed, contributing to the UHI (Forkes, 2010). Large structures may also reduce wind speeds in built up areas, inhibiting the transfer of warm air by convection (Morris, Simmonds & Plummer, 2001).

DeCarolis (2012) reported that another important property that has an effect on the intensity of the UHI is the sky view factor (SVF). Upon absorption of solar radiation, cooling occurs as outgoing long-wave radiation is released back into the atmosphere. The SVF is defined as the amount of

visible area of the sky that can be seen from a given point on the ground. It is expressed as a value between 0 (complete obstruction) and 1 (complete visibility). The sky view factor will decrease as building square footage increases, building height increases, street width decreases, and as the space between buildings decreases (Rosenzweig, Solecki & Slosberg, 2006; Unger, 2004). An inverse relationship exists between the sky view factor and the UHI, which increases as the SVF decreases. This is because large buildings that obstruct the sky view restrict the ability of surfaces to release outgoing long-wave radiation, preventing cooling from occurring (Environmental Protection Agency, 2008).

2.3.7.4 Anthropogenic heat

According to Rizwan *et al.* (2008) anthropogenic heat is generated when waste heat is produced and released into the environment as a result of human activity. Sources of anthropogenic heat include: vehicles, heating, ventilation, and air conditioning systems, appliances, industrial processes, and agricultural processes (Environmental Protection Agency, 2008).

Due to variation and changes regarding energy, transportation, and living requirements throughout the year, the quantity of waste heat released may vary diurnally, weekly, and seasonally (Rizwan, Dennis & Chunho, 2008). Studies regarding the generation of anthropogenic heat across cities have shown considerable variation in their results. For example, studies completed in Basel, Switzerland, Lodz, Poland, six cities across the United States, and Tokyo, Japan determined that annual production of waste heat was approximately 20 W/m2, 32 W/m2, 60 W/m2, and 200 W/m2, respectively (Rizwan *et al*., 2008). However, researchers believe that anthropogenic heat release has a small impact overall on the intensity of the UHI in comparison to the aforementioned causes. As a result, many mitigation strategies and recommendations concerning the UHI exclude measures to reduce the production of waste heat (DeCarolis, 2012).

2.3.7.5 Temporary Meteorological Variables

Natural factors related to meteorological patterns, geographic location and topography have the ability to exert temporary effects on the formation of urban heat islands (Environmental Protection Agency, 2008). These variables may result in diurnal, weekly, or seasonal variation with respect to the intensity of the UHI. Research has shown that the UHI is strongest on clear days with minimal cloud cover as well as on days with low wind speeds. These two conditions generally occur simultaneously during stable anticyclonic periods. Low wind speeds limit the transfer of air that promotes cooling by convection, maintaining warm temperatures in urban environments. Clear, cloudless conditions increase the temperature of the UHI by enhancing rural cooling at night. This creates a large temperature differential between rural and urban areas, where the thermal properties and structures of buildings result in comparatively slow cooling rates (Morris, Simmonds & Plummer, 2001).

Geographic location and topography may also result in changes to the UHI in different cities due to their effect on meteorology. Cities located near water bodies may experience wind patterns and convective forces that regulate heat. Additionally, topographic features such as mountain ranges may also alter weather and wind patterns, producing different UHI effects on the windward and leeward sides of mountains (Environmental Protection Agency, 2008).

2.3.8 Effects of the Urban Heat Island

2.3.8.1 Human health

The human body functions optimally at a core temperature of 37°C (98°F). Above this temperature, individuals become at higher risk for the development of heat-related illnesses, and in the worst case, mortality. The risk of experiencing these health outcomes is greatest when high temperatures occur in unison with high humidity, minimal cloud cover, and low winds. The UHI can increase the possibility of these adverse health effects occurring by significantly increasing air

temperatures above average values, impeding the body's ability to adapt and stay cool (Forkes, 2010).

As internal body temperatures rise, the risk of developing a heat-related illness, as well as the potential severity of the illness increases. At the lowest level, extreme heat can lead to general discomfort amongst individuals. However, more severe illnesses may develop as bodies lose water and vital minerals. These illnesses include heat cramps, heat rash, heat edema, fainting, heat exhaustion, and heat stroke (Forkes, 2010). Of these illnesses, heat stroke is the most severe, and the development of organ dysfunction within one year of heat stroke is a common occurrence (Chan, Lebedeva, Otero & Richardson, 2007). Extreme heat may also exacerbate and increase hospitalization rates for chronic conditions such as cardiovascular disease, respiratory disease, diabetes, renal disease, nervous system disorders, and emphysema (Chan *et al*., 2007).

In addition to the aforementioned heat-related illnesses, urban heat islands may induce heat-related mortality. Fatality is known to occur as internal body temperatures reach or exceed 105°F (Wilhelmi, Purvis and Harriss, 2004). The Centers for Disease Control and Prevention determined that from 1979-1999 excessive heat exposure resulted in 8000 premature deaths within the United States. It is interesting to note that the number of annual heat-related deaths in the United States exceeds that of all hurricanes, tornadoes, lightning, floods, and earthquakes (Environmental Protection Agency, 2008). These deaths often occur during prolonged periods of extreme heat. For example, during the 1995 heat wave in Chicago, approximately 500 individuals died, while 70,000 individuals died during the European heat wave in August 2003 (Stone, Hess & Frumkin, 2010). The European heat wave occurred due to temperatures increasing above average by approximately 3.5°C, indicating that the projected increases in temperature from climate change could significantly raise the incidence of heat-related mortality (Patz, Campbell-Lendrum, Holloway & Foley, 2005). A study of the effects of heat on mortality in Windsor indicated that from 1954-2000

approximately 37 individuals died annually due to heat-related causes. The UHI may also lead to mortality indirectly. For instance, during a heat wave in Canada in 1936, approximately 400 people died by drowning in an attempt to escape the effects of extreme heat (Health Canada, 2006).

In addition to the previously discussed direct health effects, increased temperatures have also been linked to the spread of infectious diseases. Protozoa, bacteria, and viruses, as well as disease carriers such as mosquitoes and ticks may experience improved reproduction and survival rates as temperature increases (Patz, Campbell-Lendrum, Holloway & Foley, 2005). For example, the transmission of West Nile virus by mosquitoes is known to increase following warm winters and during heat wave periods (Health Canada, 2006). While the relationship between climate change and infectious diseases is evident, the precise relationship between the urban heat island effect and infectious disease is not known. This may be an important area to research in the future as climate change intensifies the strength of the UHI.

2.3.8.2 Air quality

The impact of the UHI on air quality arises due to increased temperatures as well as through the indirect effects that greater energy demand has on increasing emissions. Increased temperatures have been correlated with the elevated production of ground level ozone (O_3), also referred to as photochemical smog. Ozone is produced by the photochemical reaction between nitrogen oxides (NOX) and volatile organic compounds (VOCs) in the presence of sunlight. Nitrogen oxides are common pollutants produced as combustion by-products, and VOCs are reactive hydrocarbon molecules that evaporate from solvents. The production of O_3 initially occurs as NO_2 separates and then combines with O_2 in the atmosphere. Under normal conditions, the reaction would reverse, however, the presence of VOCs blocks the dissociation of O_3 (Bernstein & Whitman, 2005). This reaction sequence results in the frequent issuance of smog alerts on warm summer days. Ozone is a respiratory irritant and is known to exacerbate a number of cardiopulmonary diseases including

asthma and chronic bronchitis. Studies have also linked ozone to impaired lung function and development in children (Chan *et al*., 2007).

The UHI can also indirectly contribute to poor air quality by increasing cooling demand and air-conditioning use. This can lead to increased electricity production, which may correspond to the release of greenhouse gas emissions in communities where fossil fuels are used to produce electricity. Windsor uses electricity produced from nuclear power, hydroelectric projects, renewable energy sources, and natural gas fired combined heat and power plants (Berry, Richters, Clarke, & Brisbois, 2011). However, in comparison to the combustion of coal, natural gas produces significantly lower emissions of NOX and CO_2 (Environment Canada, 2010).

2.3.8.3 Increased energy demand

Warmer surface and air temperatures during both the day and evening create an increased demand for energy. This demand is further increased by construction of urban environments with high albedo surfaces that increase the absorption of solar radiation by buildings (Forkes, 2010). Increased energy demand results from the subsequent increase in air-conditioning use in order to keep buildings at safe and comfortable temperatures. While the warmer temperatures also lower requirements for heating in the winter months, it has been demonstrated that in cities with warm summers, the high energy requirements for cooling outweigh the winter heating savings (Yow, 2007). It has been estimated that 5-10% of community electricity demand results from the need to compensate for the UHI (Environmental Protection Agency, 2008).

Greater air-conditioning use is especially concerning as it corresponds to increased peak energy demand. Peak energy demand describes the point within a 24-hour period where the demand for electricity is highest. Increases in peak energy demand may compromise the security and stability of power supplies during extreme heat events. This may result in reduced transmission efficiency or compromise the power supply entirely, leading to temporary blackouts. The most recent

blackout of significance affected multiple areas in Ontario in July 2003. These events significantly increase the risks of heat-related mortality and morbidity, as the loss of power disrupts cooling. Academic studies have determined that peak energy demand increases by approximately 2-4% for every 1°C increase in maximum temperature (Solecki *et al*., 2003).

Solecki *et al*, (2003) noted that augmented energy requirements may create a positive feedback loop that amplifies climate change and the UHI. In this scenario, increased warming may correspond to greater demands for air-conditioning use and therefore electricity generation. Electricity generation using technologies that burn fossil fuels may then lead to increases in the emissions of greenhouse gases, causing further warming in temperate areas through climate change. The UHI may also be amplified due to a greater cooling demand through the subsequent increase in the release of anthropogenic heat (Shimoda, 2003). Due to the potential to increase peak energy demand as well as GHG emissions, the World Health Organization (WHO) has identified the use of air-conditioning as an unsustainable adaptation strategy for extreme heat (Health Canada, 2006).

2.3.8.4 Aquatic ecosystem health

Aquatic ecosystem health can be negatively impacted by the discharge of runoff into surface water bodies that causes thermal shock to aquatic organisms as a result of the increase of water temperatures above normal conditions (Environmental Protection Agency, 2008). The reproduction, development, and survival of aquatic invertebrates and fish occur within an optimal range of minimum and maximum water temperatures. In particular, species within cold-water streams, rivers, and lakes may be the most vulnerable, having ecological requirements for low temperatures between 7-17 °C (Roa-Espinosa, Wilson, Norman & Johnson, 2003). High air temperatures resulting from the UHI, as well as urban form may lead to increases in water temperatures above these limits. Urban surfaces such as pavement and roofing materials absorb

large amounts of solar radiation, leading to significant increases in the temperature of runoff that flows over these areas. Surface water bodies may experience thermal shock that leads to many negative effects such as: declines in fish egg production, decreased reproductive rates, altered metabolic rates, impaired juvenile fish development, and fish lethality due to anoxia (Rossi & Hari, 2007). As a result, water bodies that are subjected to thermal shock may experience declines in species abundance and biodiversity. The precise effects that runoff will have on an aquatic ecosystem depends on the time of exposure, the critical maximum and minimum temperatures specific species can survive within, developmental stage of the species as well as the magnitude of temperature change (Rossi & Hari, 2007).

2.3.9 Mitigating the Urban Heat Island effect

DeCarolis (2012) reported that in addition to the adaptation measures that help individuals cope with the UHI, it is necessary to implement mitigation measures in order to diminish the overall intensity of the UHI. He said implementing the following measures will help to reduce the occurrence of the associated negative effects on health, air quality, water quality, and energy demand. He also observed that mitigation techniques are designed to reverse the root causes of the urban heat island effect by implementing strategies to increase albedo and emissivity, to increase cooling by evapotranspiration, and to reduce the amount of impermeable surfaces (DeCarolis, 2012). In order to achieve these objectives, potential actions within the following categories are addressed:

2.3.9.1 Cool roofs

According to Houston Advanced Research Center (2009) roofing materials comprise a significant proportion of the exposed surfaces in urban environments, at approximately 20-25%. They also absorb large amounts of solar radiation, reaching surface temperatures as high as 65.6 – 82.2°C

(150-180°F) on clear summer days. In general, commercial and industrial roofs are made from: modified bitumen, built-up roofing, or single-ply roofing materials. Residential roofs are primarily constructed using asphalt shingles.

With respect to the traditional thermal properties of roofs, they tend to have low albedo, but high emissivity, with the exception of metal roofs which also exhibit low emissivity (Environmental Protection Agency, 2008). Due to these properties, traditional roofing materials readily absorb solar radiation, heating both the surface and internal areas of buildings. This has been related to many negative implications including: elevated cooling costs, higher energy use, poor thermal comfort, and early roof deterioration (Van-Tijen & Cohen, 2008).

Unlike traditional roofs, cool roofs are built with materials that give them high albedo and high emissivity in order to minimize the absorption of solar radiation, and to maximize the release of outgoing long wave radiation (van-Tijen & Cohen, 2008). By reducing the amount of solar radiation absorbed by roofs and decreasing the surface temperature of roofing materials, cool roof applications help to minimize the UHI. Cool roof technologies have been credited with reducing roof temperatures by approximately 28-33°C during peak summer weather (Environmental Protection Agency, 2008).

2.3.9.2 Green roofs

In addition to changing the thermal properties of roofs by utilizing cool roof technologies, mitigation of the UHI and other concerns such as storm water management can be addressed through the construction of green roofs (DeCarolis, 2012). Green roofs are contained vegetation areas situated on built structures. They consist of many components including: vegetation, a growing medium, filter, drainage system, insulation, root barrier, waterproof membrane, and structural support. The precise design specifications of green roofs vary greatly between projects.

As a result, the design, construction, function, and costs associated with green roofs are also variable (DeCarolis, 2012).

The incorporation of green roofs into building design helps to reduce the UHI by increasing albedo and evapotranspiration rates. Vegetation has a higher albedo than traditional roofing materials such as asphalt shingles, tiling, concrete, gravel, and corrugated roofing, at approximately 0.70-0.85. As a result, vegetation helps to reflect a larger proportion of solar radiation, minimizing air temperatures. Additionally, plants initiate cooling by releasing water vapour into the atmosphere through evapotranspiration. During this process sensible heat is transformed into latent heat, resulting in cooling (DeCarolis, 2012).

2.3.9.3 Cool pavement

Environmental Protection Agency (2008) reported that within urban environments, paved areas account for approximately 30-45% of exposed surfaces, which causes them to have a significant impact on UHI intensity. Traditional pavement typically consists of a binder, such as asphalt or cement, as well as an aggregate, such as crushed rock. The binder serves as an adhesive, while the aggregate provides strength, resistance, and creates friction. The two most popular pavement types used currently are asphalt and impervious concrete, which can each reach high surface temperatures of 48-67°C (120-150°F). With respect to the thermal properties of asphalt and concrete, they generally have low albedo (~0.05-0.40) and high emissivity (~0.90). Due to its darker pigmentation, asphalt typically has a lower albedo, also measured as solar reflectance, than concrete. However, over time the solar reflectance of asphalt increases due to weathering, while concrete's solar reflectivity often decreases as it accumulates dirt and debris (DeCarolis, 2012).

Pavement temperatures are affected by solar radiation, solar reflectance, emittance, heat capacity, surface roughness, heat transfer rates, and permeability. Due to the low solar reflectance of both asphalt and concrete, alteration of the thermal properties of paving materials presents a

strong opportunity to reduce the intensity of the UHI. To mitigate the UHI, cool pavements can be used in order to alter the thermal and permeability properties of conventional pavement. Much of the research and development of cool pavement technologies has focused on methods that alter its solar reflectance, as this property has been determined to be the primary factor affecting the influence of pavement on UHI intensity. By increasing albedo, a greater proportion of solar radiation is reflected by pavement surfaces, resulting in cooling (DeCarolis, 2012).

The term cool pavement has also been broadened to include permeable pavement applications. The properties and structure of permeable pavement differ from other types of cool pavement which are impermeable. Permeable (porous, pervious) pavement contains void spaces that allow precipitation and stormwater runoff to infiltrate, become stored within subsurface layers, and exfiltrated beneath the earth's surface (Scholz & Grabowiecki, 2007). The presence of void spaces allows water that is stored in the pavement to evaporate, producing an effect similar to evapotranspiration that result in cooling (Global Cool Cities Alliance, 2012). Convective airflow through the pavement voids may also help to induce cooling (Environmental Protection Agency, 2008).

2.3.9.4 Urban greening

A number of studies have demonstrated the great importance of vegetation and the protection of existing green spaces and wooded areas in countering the urban heat island effect (Heisler *et al*., 1994; Taha *et al*., 1996; McPherson *et al*., 2005; Solecki *et al*., 2005). In fact, vegetation achieves cooling through various processes, more specifically:

1. seasonal shading of infrastructure;
2. evapotranspiration;
3. minimizing ground temperature differences.

Vegetation also provides other worthwhile and complementary benefits in urban areas, including:

1. improving air quality through oxygen production, CO_2 capture, filtration of suspended particulate matter and reducing energy demand for air conditioning;
2. improving water quality through retention of rainwater in the ground and soil erosion control;
3. health benefits for the population, including protection from ultraviolet (UV) radiation, reducing heat stress and providing spaces for outdoor exercise (Sundseth and Raeymaekers, 2006; Chiesura, 2004; Health Scotland *et al*., 2008; Rowntree & Nowak, 1991).

CHAPTER THREE: THE STUDY AREA AND METHODOLOGY

3.1 INTRODUCTION

This chapter consist of two sections. The first section describes the study area in terms of the location, climate, hydrology, landform, Geology, soil, settlement, education, transportation, vegetation and ecological zones, population structure and distribution, agricultural resources, minerals and industries. The second section discusses the materials and methods that were used to carried out this research work

3.2 STUDY AREA

3.2.1 Location

Katsina town is located between latitude $12^{0}30^{/}$N and $13^{0}15^{/}$N, and between longitude $7^{0}37^{/}$E and $8^{0}00^{/}$E, in the extreme part of the state. Katsina Local Government Area (LGA), in which Katsina city is located shares boarder with the LGAs of Kaita to the north, Rimi and Batagarawa to the east and south, and Jibia to the west (See fig 3.1). The creation of Katsina State with the capital located in Katsina brought a very remarkable town expansion. Presently, Katsina metropolitan city has extended into Batagarawa LGA along Kano, Dutsinma and Batsari roads, and Jibia LGA around the Army Barracks. The town is about 50km to the Nigerian border with Maradi, Republic of Niger.

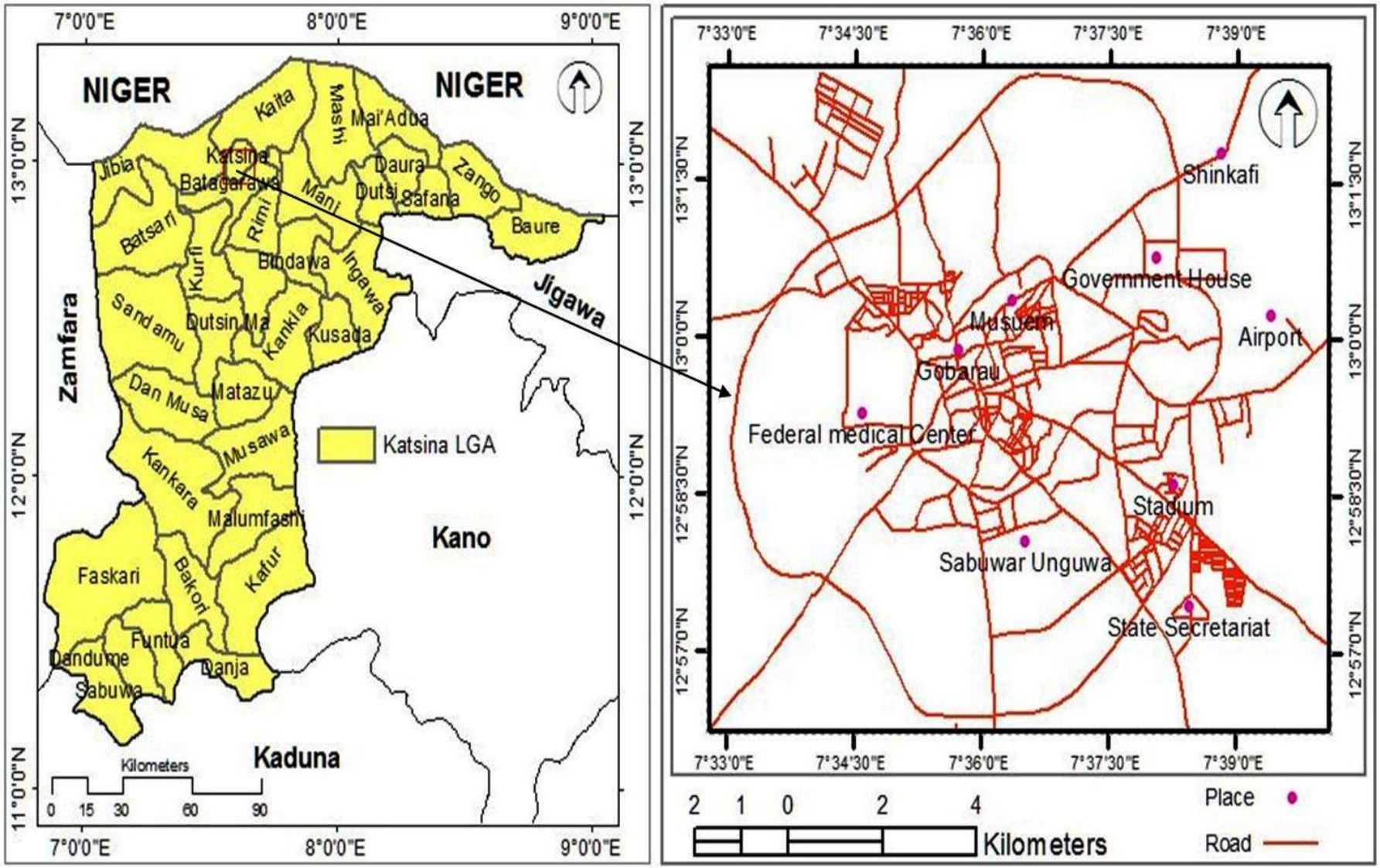


Figure 3.1: Map of the Study Area

3.2.2 Climate

. The climate of Katsina is Tropical Continental type that is hot and dry for most of the year. Maximum day temperatures of about 38^0C in the months of March, April and May are common and the minimum temperature is about 22^0C in the month of December and January (Rumah and Sheikh, 2010). According to Oguntoyinbo (1984) in Nigeria, sunshine hours range from minimum of 1,300 hours in Niger Delta to over 3,200 hours in the extreme north-east on annual basis (Oguntoyinbo, 1984)

Rainfall in Katsina Metropolis, as for the whole country, is a good reflection of the seasonal variations of the Inter-Tropical Discontinuity (I.T.D) and it falls mainly between May and September. It ranges between 0.0 to around 800mm. Rain falls in Katsina metropolis when the wind blows to Northeast from Southwest while the reverse brings dryness. North-easterly wind blowing from north-east is associated with continental tropical air mass and brings no rain, while south-westerly wind blowing from south-west is associated with maritime tropical air mass which is wet and brings rain as it originates from the sea, Atlantic Ocean (Gide, 2012).

3.2.3 Hydrology

The main river draining the town is River Ginzo, which passes through the town and move northwards. Drainage pattern of the area is dendritic to sub-parallel and northward in direction, with widely space drainage lines. Stream flow in the area strongly reflects the climatic environment and, in particular, the season and torrential nature of the rainfall. Thus, three main types of stream flow pattern have been recognized in the area (Danbuzu, 2012);

i. Perennial flows: Low dry season discharges with flash floods superimposed on high rainy season discharges. This flow pattern occurs on the largest river i.e. Ginzo and major tributaries.

ii. Seasonal flow: Zero dry season flow, flash floods superimposed on rainy season flow which may be high or low depending on catchments area. The river along which Tille is located to this category

iii. Flash flow only i.e., there is flowing water in the stream channel only during and for a short while after run-off producing storms.

The alluvial sediments in the flood plains, which range from gravels to clay with coarser material along present and old river beds, become saturated during the rainy season and may drain away along the river course during the dry season or, become dammed by impervious rock or clay barriers (Danbuzu, 2012).

3.2.4 Landform

The Landforms reflects the sedimentary rock formation of the area. The landscape is relatively flat, almost featureless, typically less than two degrees, and of about 510m at the Katsina city center (MLSK, 2008). The plain is underlain by clayey sandstones and grits with small basal pebble. Rock-out crops are generally absent, other than into the small inliers of Basement complex. Laterite capping only occur frequently and drainage texture is considerably much coarser than on basement complex plains further south of the area (Zayyana, 2010).

3.2.5 Geology

The continental sediments of Katsina plains consist of feldspatic clayey sandstones and grits with small basal pebble beds. The sediments have maximum thickness of about 100m and the regional dip is to the north-west. The sediments thin to the south and, in places, only the pebble beds remain on the higher interfluves. The southern boundary is diffuse and outliners are frequent, south of the main body. The sediments have been equated with the Gundumi formation of the Lullummenden Basin and are therefore mid cretaceous in age

(Ologe, 1985).

Alluvial deposits are associated with the present valleys. The older alluvium, which is partly colluvial in origin, forms a valley fill and may be contemporaneous with a high terrace found along Ginzo River. Aeolian deposits overlie the older alluvium. The Aeolian mantle lacks definite pattern and also shows a marked variation in thickness. The younger alluvium occurs along the Tille River within the present floodplain. Recent alluvium deposits are associated with the present floodplain of the major rivers in the area (Ologe, 1985).

3.2.6 Soil

Soils in the area, as elsewhere in Nigeria, represent an interface between intensive chemical weathering of rocks, and an active and intermittent surface and subsurface denudation system, fuelled by intensive rainfall and rapid runoff. The properties of the soils, therefore, represent complex interrelationships between intensity of weathering and rate of lateral and vertical eluviations of materials, which are in turn related to lithology, topography, climate, vegetation and other environmental controls (MLSK, 2008).

The soil of the study area fall under tropical ferruginous soils ((Alfisols) and weakly developed alluvial soils (Hydromorphic soil) of the major streams. These soils are found on recent sediments of varying ongm, or older Aeolian sediments which have either been redistributed by erosion or which have evolved under a semi-arid climate and show no characteristics of the ferruginous tropical features associated with seasonal water logging so that many have hydromorphic tendencies and grade into major soil group (MLSK, 2008).

3.2.7 Vegetation

Lying within the Northern Sudan savanna, the vegetation is dominated by fine-leaved Acacia spp. and their associates. These trees include Adonsonia digitata, Parkia bigloboza, Anogeissum leiocarpus, Afrormosia laxiflora, Bombax costatum, Boswellia dalzielii, Burkea africana etc. The common shrub and shrubby species include Annona senegalensis, Bridelia ferruginea, Gardenia spp, Grewia mollis, Hymenocardia acida, Lannea kerstingii, May tenus senegalensis, Nauclea latifolia, Pillostigma thonningii etc (Danbuzu, 2012).

The trees characteristically grow long tap roots and thick barks both of which make it possible for them to withstand the long dry season and bush fires. The grass cover is mostly perennial, with durable roots, which remain underground after stalks are burnt away or wilted in the dry season only to germinate with the first rains. The precise and mixture of the various species is determined by such factors as soil type, moisture conditions, and the degree of human disturbance. The main physiographic communities encountered in order of importance are: cultivated parkland, shrub savannah and floodplain grassland. This biodiversity has been strongly modified as a result of urban expansion and construction (MLSK, 2008).

3.2.8 Population Structure and Distribution

Urban Katsina has a fairly large population, enjoys Sub-Sahara African rate of population increase with average birth and death rates of 4.2% and 1.6% respectively (Zango, 2010). As of 1952 census, the population figure was 52,672 and rose to 223,644 in 1991, by then it had already acquired the status of a state capital. The population figure after the 2006 census was recorded to be 327,376 (National Population Commission, 2006).

3.2.9 Settlement

The settlement pattern has characterized by two categories base on population density. The first category is the high to medium density settlement s which include the Cikin Birni (Old City) with their peripheral areas respectively. While the second category is the low density settlements of Government Reservation Areas (GRA), Kofar Marusa Low Cost and the New Layout among others. The Cikin Birni which is the old city and the most densely populated and the most densely populated area in the metropolis have a unique cultural setting that affects the people in the area. Most buildings are made up of mud and clay, closely packed together and surrounded with walls (Hassan, 2008).

3.2.10 Land Uses

Land use in the study area is dominated by urban activities, such as residential, institutional, commercial and industrial land uses, with small area mostly undeveloped for farming. Aside from major urban land uses mentioned above, other land uses such as livestock production and gathering are also carried out in the area. Residential area cover most part of the study area, different land uses such as commercial, institutional, and educational are all located within the residential areas. Sabuwar Unguwa extension is the major area functioning as industrial layout. Industries such as steel rolling, packaging, beverages processing etc are found in this area. Commercial activities happened to be growing very fast in the area. There are many smalls and one major central market (Danbuzu, 2012).

The popular markets here are Katsina central market, Kofar Marusa market and the old market (Tsohuwar Kasuwa). Also there are many departmental stores, shopping centres and supermarkets- where local, national and foreign commodities are sold. Institutional land

uses can be found at various locations within urban Katsina. Tertiary institutions include Umaru Musa Yar'adua University, Federal College of Education, Hassan Usman Katsina Polytechnic, and School of Nursing and Midwifery in addition to numerous nursery/primary and secondary schools both governmental and privately owned (Danbuzu, 2012).

Agricultural activities are confined to open spaces within the built-up areas and at suburb, and on the stretches of flood plains and the little floodable plains of the little floodable part of the low terrace depressions that retains water in the area and other undeveloped lands within the area and other extensive areas just outside the city. The most common market gardening crops grown are Okra, Cabbage and Spinach etc. The area also supports large number of cattle, sheep and goats. All livestock in the area graze on natural pastures and shrubs for their nutritional needs, and supplementary feeding from the owners. Gathering of non timber forest products (NTFPs) form a small but important part of human activities in the area. Such items provide subsistence goods and services, as well as items of trade. Throughout the area, plant medicines are used for both curative and preventive treatments. Fuel wood constitutes the main energy source for cooking. Besides, gathering processing and trading of the products provides a good source of supplementary income to many households in the area (Zayyana, 2010).

3.3 METHODOLOGY

3.3.1 Reconnaissance survey

Reconnaissance survey was carried out in order to have a general knowledge of the study area. This knowledge is very useful during visual image interpretation process before and after image classification.

3.3.2 Types and Sources of Data

The data and materials that were used to carry out this study are as follows:

3.3.2.1 Satellite Imagery

Date Acquired	**Satellite**	**Sensor**	**Spatial Resolution (m)**	**Path/Row**	**Format**
24-11-1986	Landsat 5	TM	Bands 1-5,7: 30x30 Band 6: 60x60	189/51	GeoTIFF
19-10-1999	Landsat 7	ETM	Bands 1-5,7: 30x30 Band 6: 60x60	189/51	GeoTIFF
20-10-2014	Landsat 8	OLI_TIRS	Bands 2-7: 30x30 Bands 10: 100x100	189/51	GeoTIFF

Table 3.1: Description of Landsat image data
Source: Satellite Imageries Metadata

All the three satellite imageries were downloaded from the United States Geological Survey (USGS) website, www.glovis.usgs.gov. See fig 3.2, 3.3, 3.4, 3.5, 3.6 and 3.7

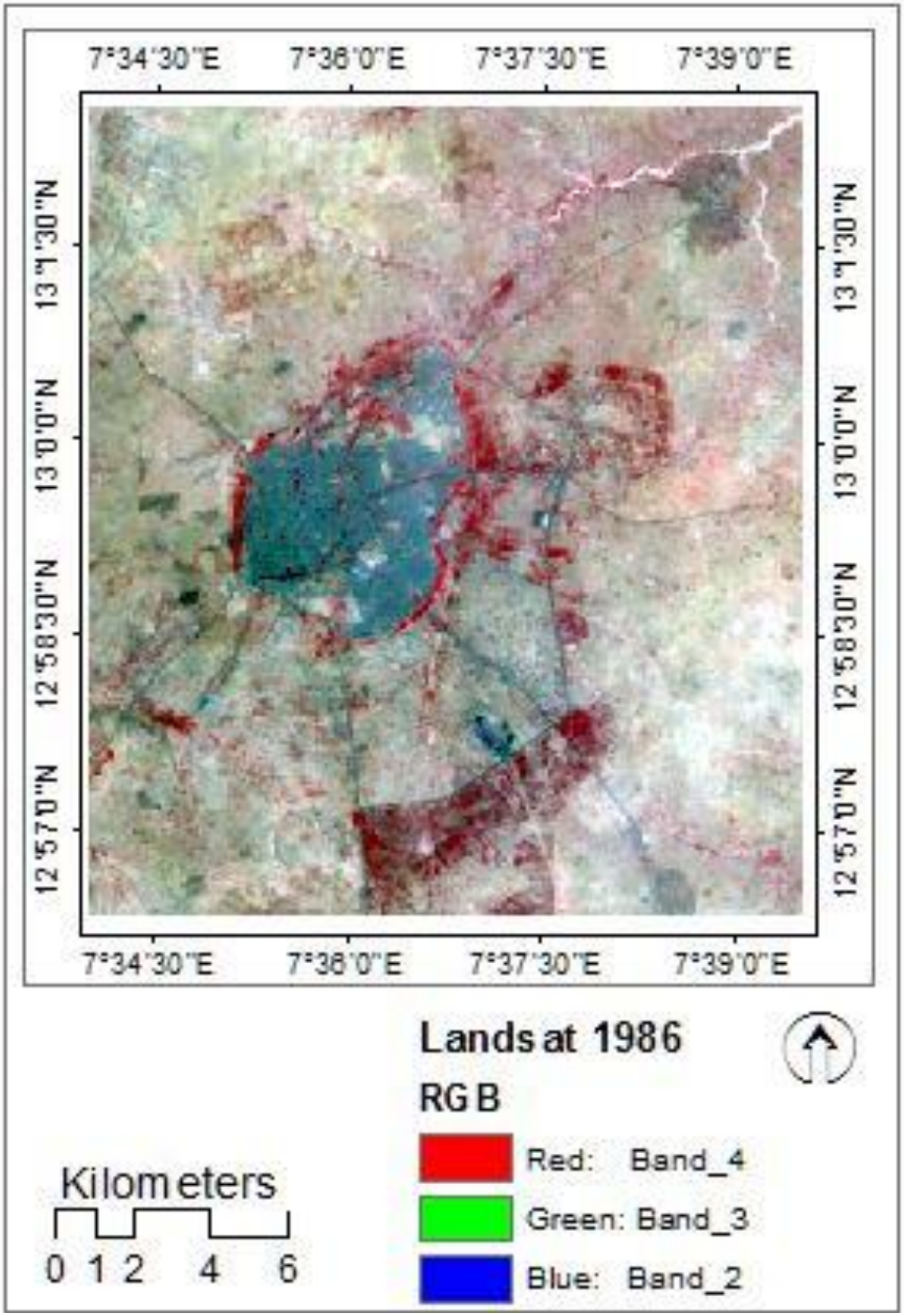


Fig 3.2: 1986 False Colour Composite (4,3,2) Landsat image of the study area

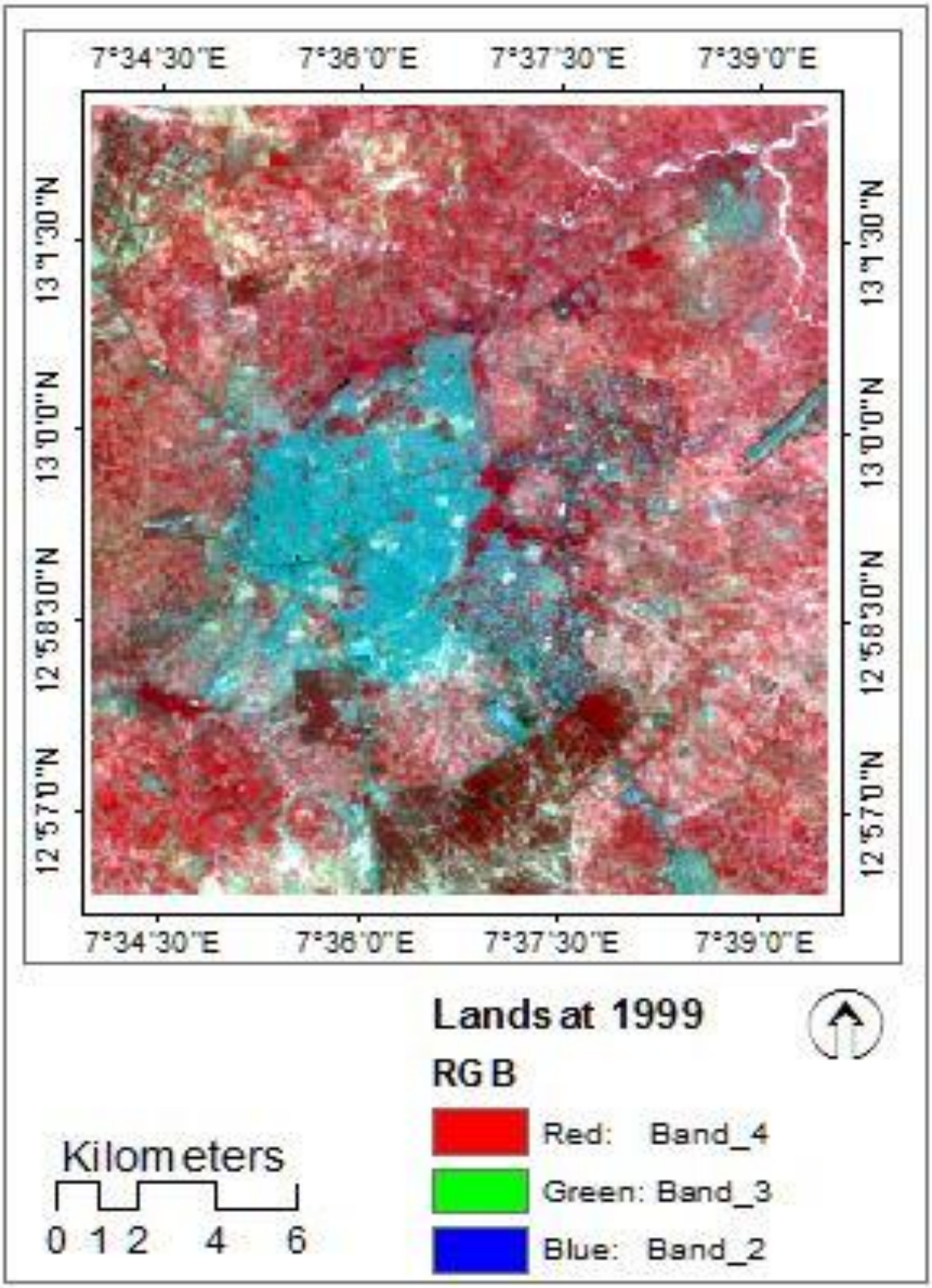


Fig 3.3: 1999 False Colour Composite (4,3,2) Landsat image of the study area

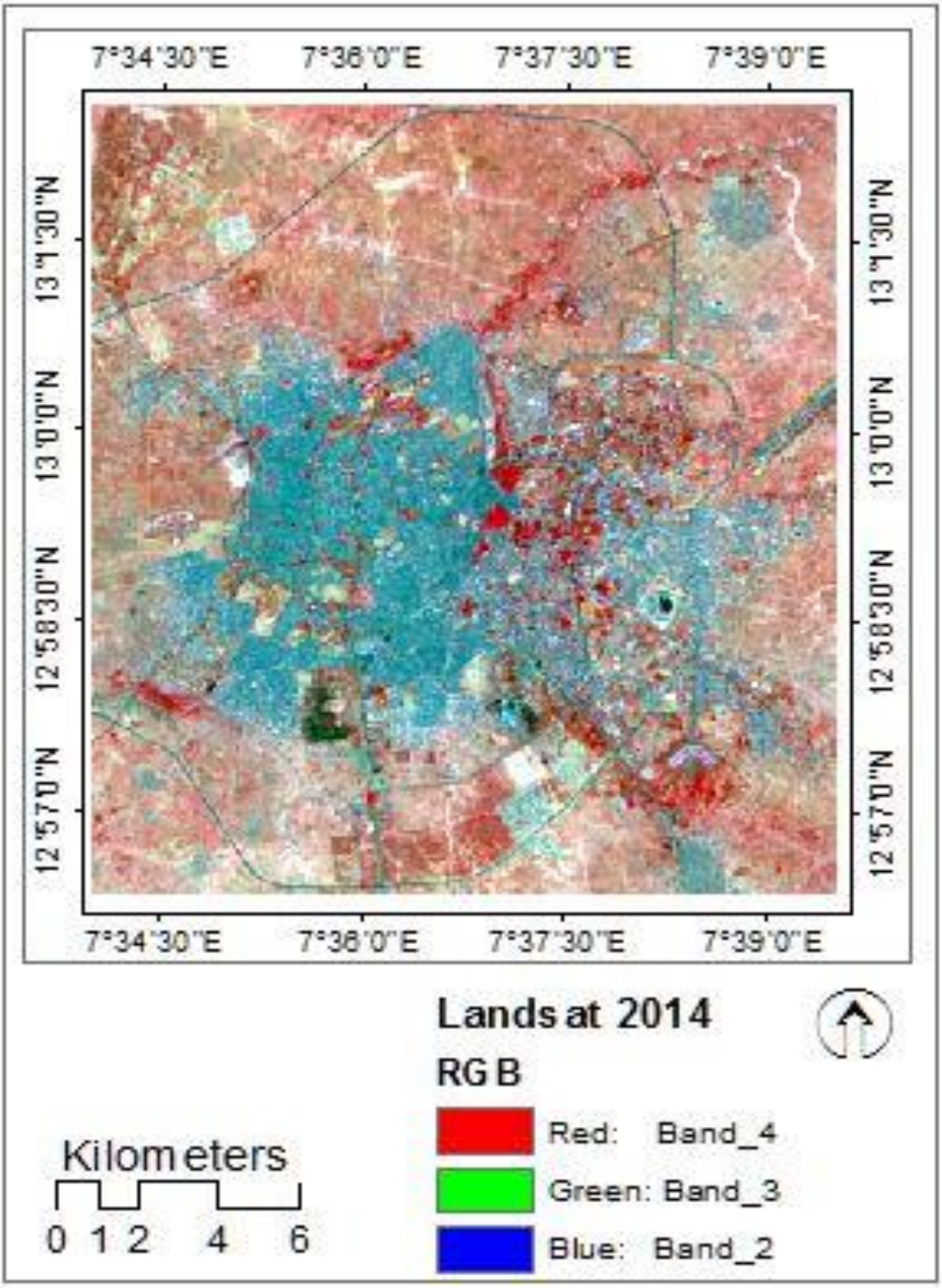


Fig 3.4: 2014 False Colour Composite (4,3,2) Landsat image of the study area

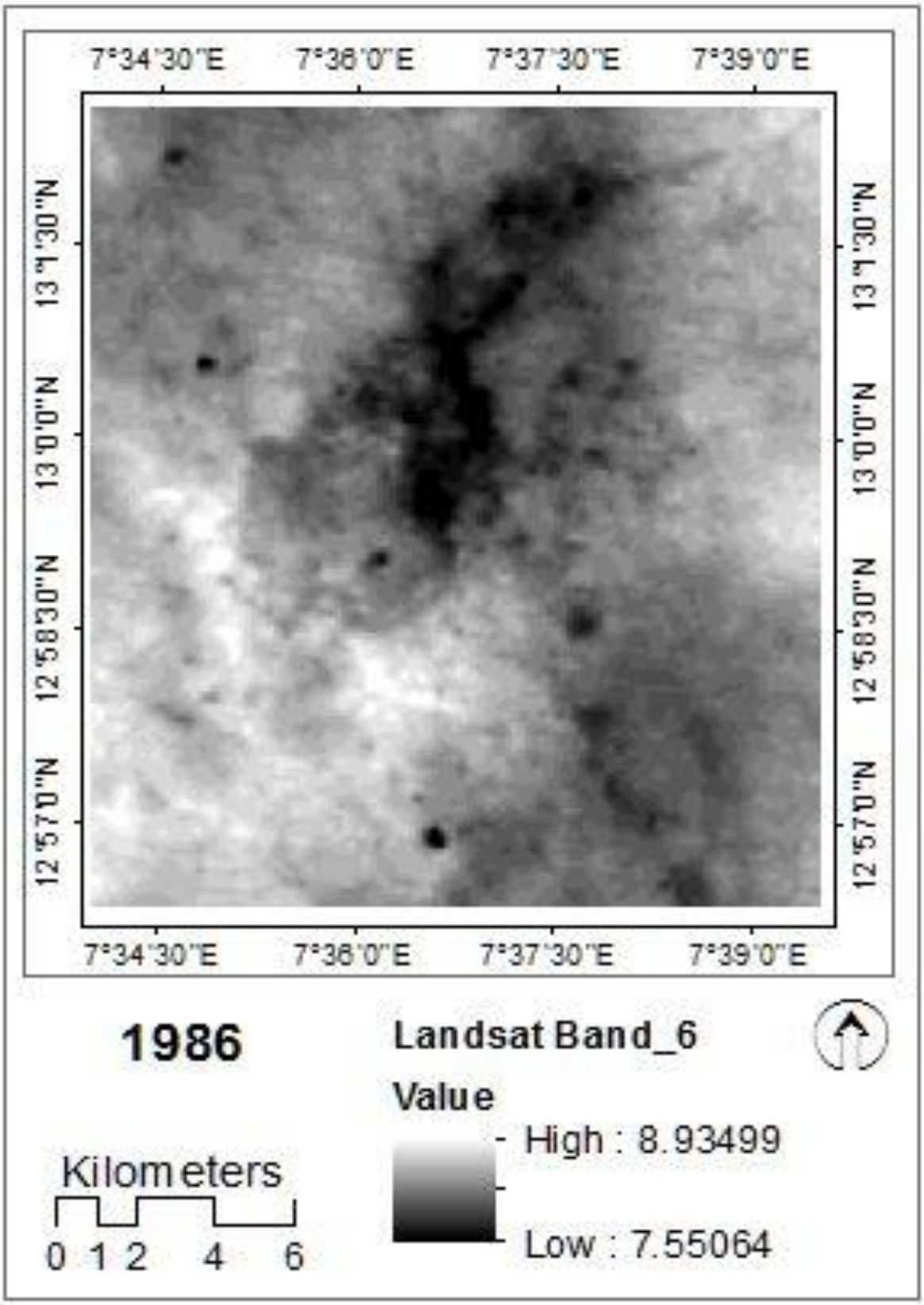


Fig 3.5: 1986 thermal Infrared band of the study area

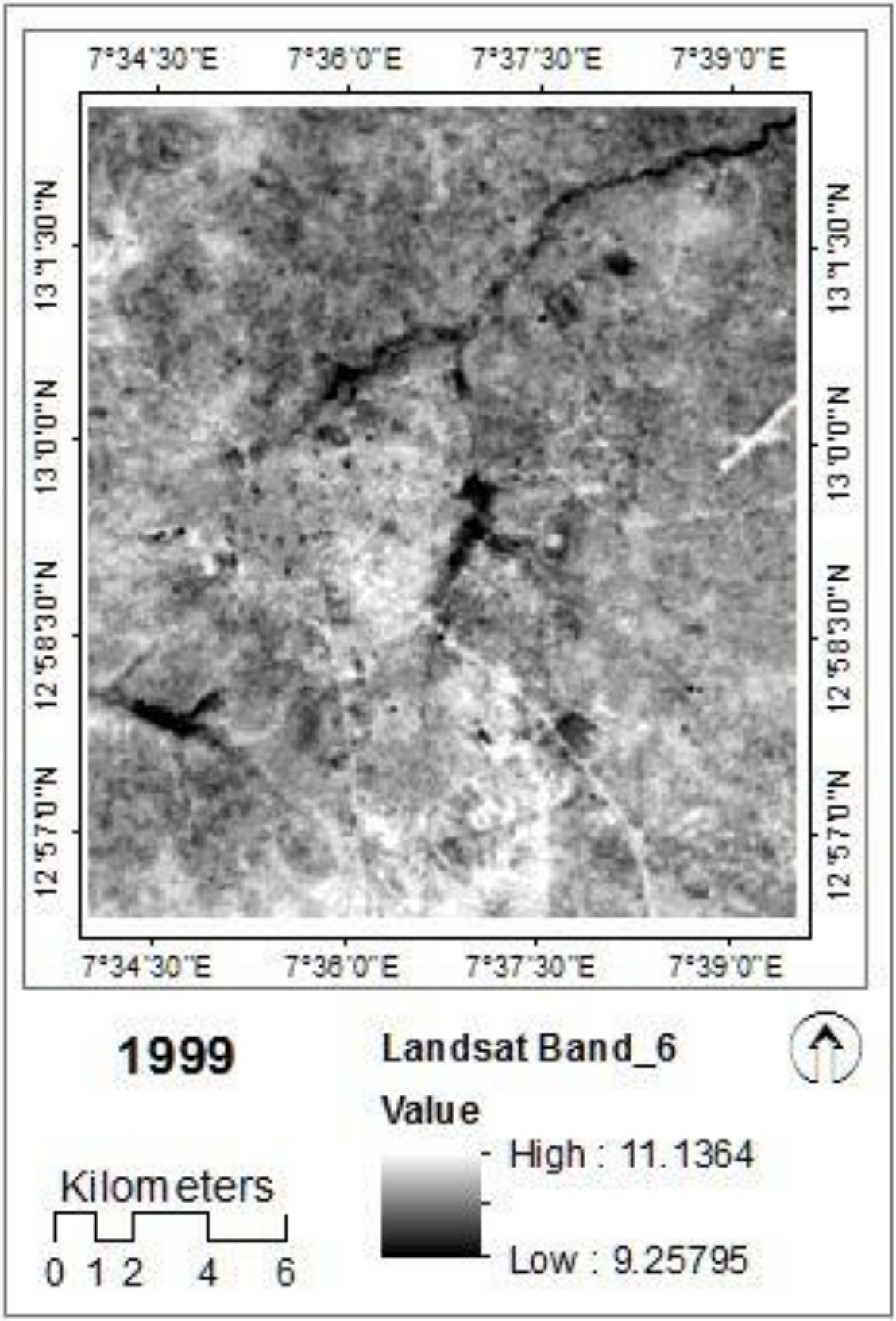


Fig 3.7: 1999 thermal Infrared band of the study area

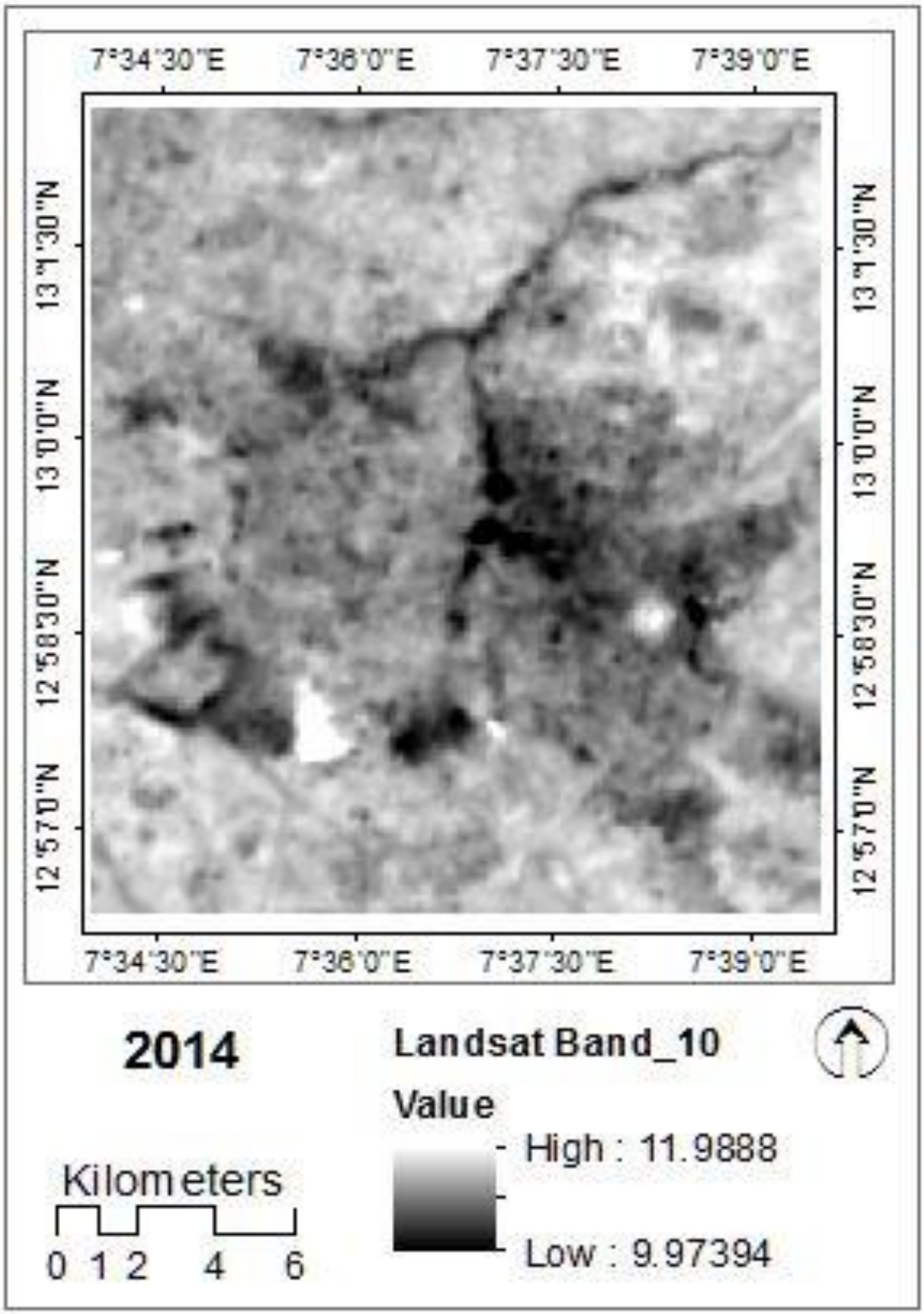


Fig 3.7: 2014 thermal Infrared band of the study area

3.3.3 Hardware and Software

3.3.3.1 Hardware

High speed memory digital electronic computer hardware Hewlett Packard (HP) Pavilion G62 laptop was used.

3.3.3.2 Software

ERDAS Imagine 9.2, ArcGIS 10.1 and Microsoft office 2007 (word and Excel) were used. Erdas Imagine 9.2 was used for image processing and analysis. ArcGIS 10.1 was used for data preparation and map composition. Microsoft office (Word and Excel) was used for reporting and analysis.

3.3.4 Methods of Data Analysis

3.3.4.1 Image Pre-processing

Landsat TM image for 1986, ETM for 1999 and OLI_TIRS image for 2014 were used in this study. All images were preprocessed by the U.S. Geological Survey (USGS) National Center for Earth Resources Observation and Science (EROS) to correct radiometric and geometrical distortions of the images to level 1G products.

All the bands were utilized at a spatial resolution of 30m. These spectral bands were layer stacked to produce a composite image of the study area for each year (1986, 1999 and 2014) for the purpose of land use/land cover classification and image analysis. Thermal band 6 for Landsat 5 TM, ETM and band 10 for Landsat 8 TIRS were used to extract the surface temperature from all the periods under consideration. The composite images and thermal bands were clipped with a rectangular area of interest in Erdas Imagine 9.2

The thermal bands had their original pixel sizes of 120m for TM and 100m for TIRS images were resampled to 30m using the nearest neighbour algorithm to match the pixel size of other spectral bands.

3.3.4.2 Supervised image classification

In order to examine the effects of human activities in the study area, a land cover classification is necessary for detection of LULC changes as a result of rapid urbanization from 1986 to 2014. The categories or classes considered were Farmland, Vegetation, Bareland and Built up. After selecting training areas, a supervised classification with the maximum likelihood algorithm was conducted to classify the Landsat images using bands 2 (green), 3 (red) and 4 (near infrared). Visual image interpretation was done with field knowledge and making reference to Google earth images of the study area. The error matrixes of the three land use and land cover maps were generated to assess the accuracy of the classification result.

3.3.4.3 Accuracy Assessment

Land cover maps derived from classification of images usually contain some sort of errors due to several factors that range from classification techniques to methods of satellite data capture. Therefore, evaluation of classification results is an important process in the classification procedure. The accuracy assessment was done by generating 200 equal random points for the classified images, using the accuracy assessment tool in Erdas Image. The error matrix was generated using the same accuracy assessment tool in Erdas Imagine by comparing the randomly selected pixels with the corresponding referenced data.

3.3.4.4 Change detection analysis

The change detection algorithm employed for detecting land use and cover change was image differencing. Image differencing is one of the widely used change detection approaches and is

based on the subtraction of images acquired in two different times. In the process, the digital number (DN) value of one date for a given band is subtracted from the DN value of the same band of another date (Singh, 1989). Change detection analysis was carried out to evaluate the changes in land use/land cover and surface temperature intensity from 1986, 1999 and 2014 classification and surface temperature maps of the study area.

3.3.4.5 Conversion of the digital number (DN) to spectral radiance (L_λ)

The following equation was used to convert the digital number (DN) of TIR bands of Landsat data into spectral radiance (Landsat 7 Science Data User's Handbook, 2002):

$$L_\lambda = ((LMAX_\lambda - LMIN_\lambda)/(QCALMAX - QCALMIN))*(QCAL - QCALMIN) + LMIN_\lambda \quad (1)$$

where:

L_λ *= Spectral Radiance at the sensor's aperture in watts/(meter squared * ster * µm)*

QCAL = the quantized calibrated pixel value in DN

$LMIN_\lambda$ *= the spectral radiance that is scaled to QCALMIN in watts/(meter squared * ster * µm)*

$LMAX_\lambda$ *= the spectral radiance that is scaled to QCALMAX in watts/(meter squared * ster * µm)*

$QCALMIN_\lambda$ *= the minimum quantized calibrated pixel value (corresponding to* $LMIN_\lambda$*)*

$QCALMAX_\lambda$ *= the maximum quantized calibrated pixel value (corresponding to* $LMAX_\lambda$*).*

See Table 3.3 for the values of $LMAX_\lambda$, $LMIN_\lambda$, $QCALMAX_\lambda$ *and* $QCALMIN_\lambda$

3.3.4.6 Conversion of spectral radiance to temperature in Kelvin

To convert the spectral radiance values to brightness temperature, the equation below was used (Landsat 7 Science Data User's Handbook, 2002):

$$T_k = K_2 \div \ln (K_1 \div L_\lambda + 1) \quad (2)$$

Where T_k is effective at-satellite temperature in Kelvin, L_k is spectral radiance in W/(m^2 ster μm); and K_2 and K_1 are pre-launch calibration constants. See Table 3.3 for values of K1 and K2.

3.3.4.7 Conversion of Kelvin to Celsius

The final apparent surface temperature in Celsius (˚C) was calculated with the following equation:

$$T_c = T_k - 273.15 \quad (3)$$

Where T_c is the temperature in Celsius (˚C), T_k is the temperature in Kelvin (K).

Satellite	Year	Band	$LMAX_\lambda$	$LMIN_\lambda$	$QCALMAX_\lambda$	$QCALMIN_\lambda$	K1	K2
Landsat5	1986	6	15.303	1.238	255	1	607.76	1260.6
Landsat7	1999	6L	17.04	0	255	1	666.09	1282.7
Landsat8	2014	10	22.0018	0.1003	65535	1	774.89	1321.1

Table 3.3: Parameters for the Calculation of surface temperature

3.3.4.8 Estimation of surface temperature of land use land cover types

In order to estimate the surface temperature of land use/cover types, 100 sample points were selected randomly from each land use land cover types in the study area. Geographic link and enquire cursor tools of Erdas imagine 9.2 were used to investigate the ST value of each sample point randomly selected. The average ST value for each land use land cover was calculated by taking the arithmetic mean of the values for each land use land cover.

CHAPTER FOUR: RESULTS AND DISCUSSIONS

4.1 INTRODUCTION

This chapter presents and discusses the results of this study. The first and second parts are on land use/ land cover classification and the evaluation of land use/ land cover maps respectively. The third section is on surface temperature computation while the fourth is on the relationship between surface temperature and land use/ land cover. The results are presented in form of maps and statistical table.

4.2 LAND USE LAND COVER MAPPING

Land use land cover maps for the three years of the study were generated and presented in Fig. 4.1, 4.2 and 4.3.

4.2.1 Land use Land Cover Classification

Table 4.1 summarises the total land area for each land use land cover class across the study area and the corresponding percentage of the total.

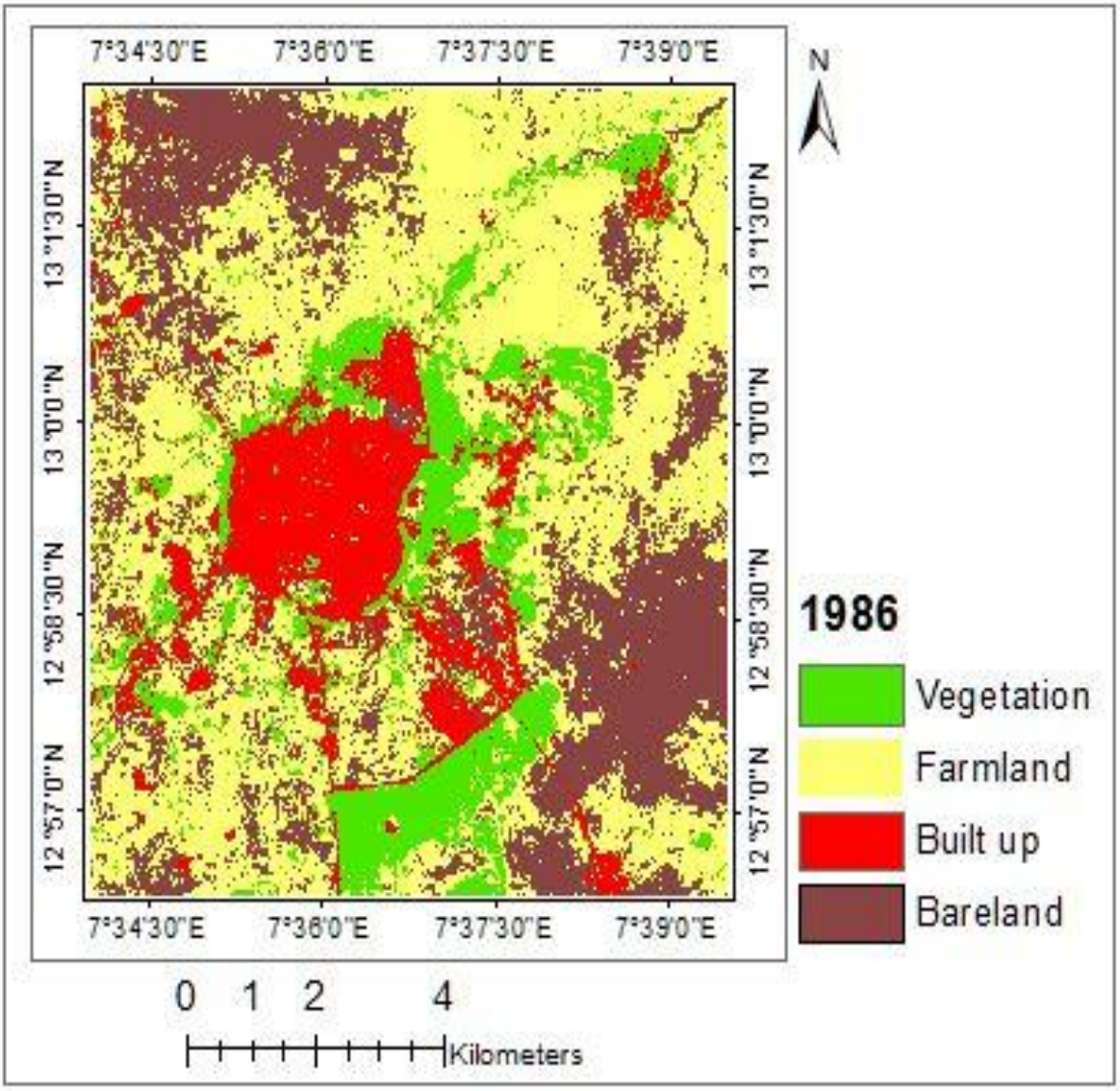


Fig. 4.1: 1986 Land use Land Cover Classification map of the Study area
Source: Author's GIS analysis (2014).

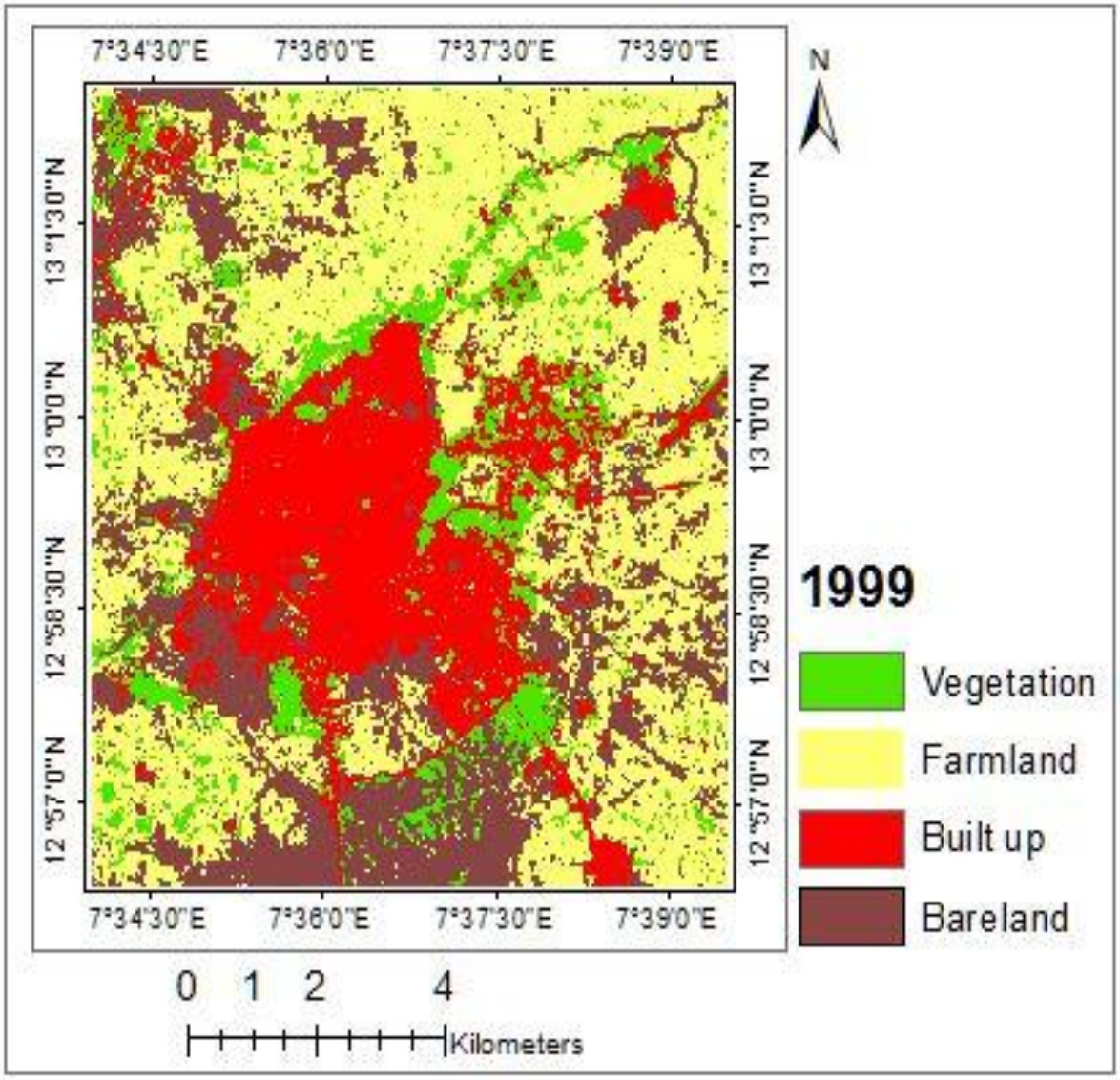


Fig. 4.2: 1999 Land use Land Cover Classification map of the Study area
Source: Author's GIS analysis (2014).

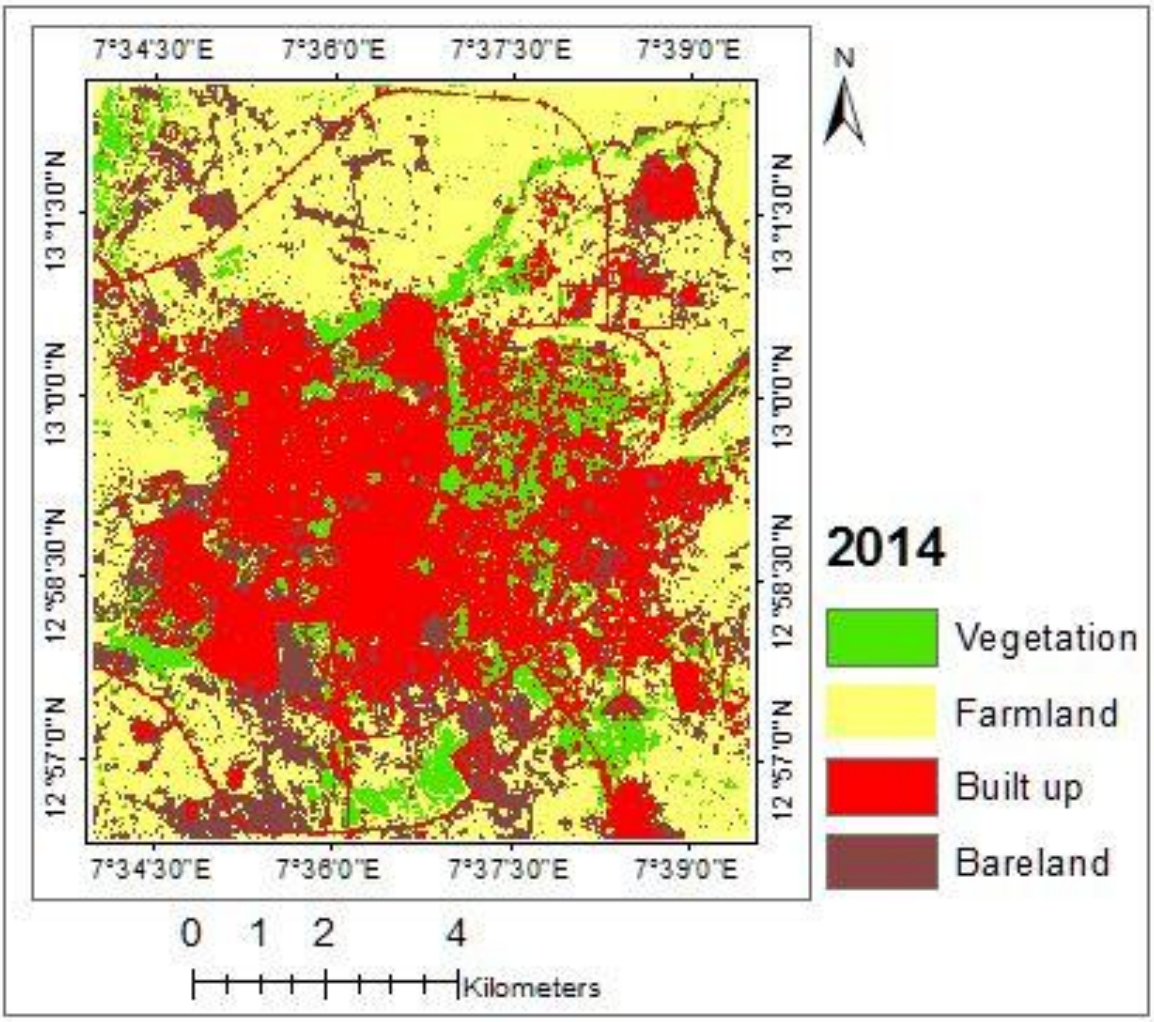


Fig. 4.3: 2014 Land use Land Cover Classification map of the Study area
Source: Author's GIS analysis (2014).

Table 4.1: Land use Land Cover Statistics

Class	1986		1999		2014	
	Area (ha)	**Area (%)**	**Area (ha)**	**Area (%)**	**Area (ha)**	**Area (%)**
Farmland	5359.6	46.8	4938.0	43.1	4610.5	40.3
Vegetation	1586.4	13.9	1322.2	11.5	1248.9	10.9
Bareland	3018.2	26.4	2823.8	24.7	1991.0	17.4
Built up	1484.3	13.0	2364.6	20.7	3598.1	31.4
Total	**11448.5**	**100.0**	**11448.5**	**100.0**	**11448.5**	**100.0**

Source: Author's analysis (2014)

The land use land cover classification for 1986 from TM satellite image (fig. 4.1) indicates that most of the study area was under farmland accounting for 5359.6 ha (46.8%), followed by bareland which occupied 3018.2 ha (26.4%), while vegetation and built up amounted to 1586.4 ha (13.9%) and 14.84.3 ha (13%) respectively.

The image classification result generated from 1999 Landsat ETM (fig. 4.2) shows that farmland still remains the major land use land cover but with a decrease to 4938.0 ha (43.1%) of the total area. Bareland has decreased to 2823.8 ha (24.7%) while built up has increased to 2364.6 ha (20.7%). Vegetation has also decreased to 1322.2 ha (11.5%).

Results generated from 2014 LandSat8_OLI image (fig. 4.3) showed that the dominant class is farmland, even though it has decreased slightly to 4610.5 ha (40.3%). Built up increased significantly to 3598.1 ha (31.4%), while bareland and vegetation decreased to 1991.0 ha (17.4%) and 1248.9 ha (10.9%).

4.2.2 Accuracy Assessment of Image Classification

Evaluation of classification results is an important process in satellite image classification procedure. This is necessary to ascertain the level of correctness and reliability of the classification

output. Kappa statistics/index which provides a more rigorous assessment of classification accuracy was also computed for each classified map. The Kappa coefficient expresses the proportionate reduction in error generated by a classification process compared with the error of a completely random classification. Table 4.2, 4.3 and 4.4 show the accuracy assessment of 1986, 1999 and 2014 image classification results respectively.

4.2.2.1 Accuracy assessment of image classification landsat TM (1986)

Table 4.2: Error matrix of 1986 Image Classification

	Vegetation	Farmland	Bareland	Built up	Kappa	Producer's accuracy	User's accuracy
Vegetation	91	5	0	4	0.88	90%	91%
Farmland	4	86	10	0	0.81	81%	86%
Bareland	1	13	81	5	0.75	86%	81%
Built up	5	2	3	90	0.87	91%	90%
Total	101	106	94	99			

Overall Classification Accuracy = 87%

Overall Kappa Statistics = 0.83

Source: Author's GIS analysis (2014)

Landsat TM image 1986 was classified into 4 land use land cover categories. Farmland was classified with lower producer's accuracy (81%) than other classes. This is as a result of errors particularly mixing with bareland. Built up, vegetation and bareland were classified with higher producer's accuracy of 91%, 90% and 86% respectively. The overall classification accuracy of the image was 87% while the overall Kappa coefficient was 0.83

4.2.2.2 Accuracy assessment of image classification landsat ETM. (1999)

Table 4.3: Error matrix of 1999 Image Classification

	Farmland	Vegetation	Bareland	Built up	Kappa	Producer's accuracy	User's accuracy
Farmland	89	7	4	0	0.85	87%	89%
Vegetation	3	90	1	6	0.87	90%	90%
Bareland	10	1	88	1	0.84	93%	88%
Built up	0	2	2	96	0.95	93%	96%
Total	102	100	95	103			
Overall Classification Accuracy = 91%							
Overall Kappa Statistics = 0.88							

Source: Author's GIS analysis (2014)

Landsat ETM image (1999) was also classified into 4 land use land cover categories with higher producer's accuracies. Built up and bareland have the same producer's accuracy of 93% while vegetation and farmland have 90% and 87% respectively. The overall classification accuracy was much better (91%) and the overall Kappa coefficient was 0.88

4.2.2.3 Accuracy Assessment of Image Classiffication Landsat 8 OLI (2014)

Table 4.4: Error matrix of 2014 Image Classification

	Farmland	**Vegetation**	**Bareland**	**Built up**	**Kappa**	**Producer's accuracy**	**User's accuracy**
Farmland	91	4	5	0	0.88	86%	91%
Vegetation	8	77	5	10	0.71	90%	77%
Bareland	6	1	85	8	0.80	81%	85%
Built up	1	4	10	85	0.80	83%	85%
Total	106	86	105	103			

Overall Classification Accuracy = 85%

Overall Kappa Statistics = 0.79

Source: Author's GIS analysis (2014)

In the classification of Landsat8_OLI image (2014), the producer's accuracy of bareland (81%) was lower than other classes. This is as a result of error due to omission and misclassification to farmland, vegetation and built up. Lower producer's accuracy was also observed for built up (83%) due to omission and misclassication to vegetation and bareland. The overall classification accuracy was 85% while the Kappa cofficient was 0.79.

4.3 LAND USE LAND COVER CHANGE

Table 4.5: Land Use Land Cover Change Statistics

Class	1986-1999			1999-2014			1986-2014		
	Change (ha)	(%)	Growth (%/yr)	Change (ha)	(%)	Growth (%/yr)	Change (ha)	(%)	Growth (%/yr)
Farmland	-421.6	-7.9	-0.6	-327.5	-6.6	-0.4	-749.1	-14.0	-0.5
Vegetation	-264.2	-16.7	-1.3	-73.3	-5.5	-0.4	-337.5	-21.3	-0.8
Bareland	-194.5	-6.4	-0.5	-73.3	-2.6	-2.0	-1027.3	-34.0	-1.2
Built up	880.3	59.3	4.6	1233.5	52.2	3.5	2113.8	142.4	5.1

Source: Author's analysis (2014)

According to Table 4.5, from 1986 to 1999 farmland, vegetation and bareland decreased by 421.6 ha (7.9%), 264.2 ha (16.7%) and 194.5 ha (6.4%) respectively, while the built up environment increased by 880.3 ha (59.3%). This may be due to the change in the status of Katsina town from a local government area headquarters to a state capital when Katsina state was created in 1987. Similarly, during the second period between 1999 and 2014 farmland decreased by 327.5 ha (6.6%), vegetation by 73.3 ha (5.5%) and bareland by 73.3 ha (2.6%). However, the built up environment increased by 1233.5 ha (52.2%). In general, between 1986 and 2014 farmland, vegetation and bareland decreased by 749.1 ha (14%), 337.5 ha (21.3%) and 1027.3 ha (34.0%) respectively while the built up area drastically increased by 2113.8 ha (142.4%) with the greatest increase occurring from 1999 to 2014, 59.3% within a period of 13 years as compared with 52.2% within 15 years between 1999 and 2014.

The annual growth rate in built up as determined by the land use land cover change statistics was 4.6% from 1986 to 1999, 3.5% from 1999 to 2014 and 5.1% for the entire period of 1986 to 2014. This implies a dramatic urban growth and change in the morphology of the city size and extents. This was as a result of increase in housing (i.e. settlements) and infrastructural development such

as health, educational and other socio-economic reasons. On the other hand, farmland showed an annual reduction rate of 0.6% from 1986 to 1999, 0.4% from 1999 to 2014 and an overall annual reduction rate of 0.5% for the entire study period of 1986 to 2014. Similarly, vegetation also experienced an annual reduction rate of 1.3% from 1986 to 1999, 0.4% and 0.8% for the entire study period of 1986 to 2014. Bareland decreased annually at the rate of 0.5% from 1986 to 1999, 2.0% from 1999 to 2014 and 1.2% for the entire study period of 1986 to 2014. These results corroborate the findings of Abdulkadir (2009) in which he used geomatics technology to analyze the pattern of spatial growth in Katsina metropolis.

In general, the land use land cover change statistics in Table 4.2 indicates that increase in built up area mainly emanated from conversion of other land uses and land covers especially farmland to built up area during the past 28 years (1986-2014) as a result of rapid urban growth within the metropolis. Besides the land use land cover change statistics, graphical representations of the image classification result and visual comparison offer a general insight into the magnitude of the defined classes across the landscape and the changes observed (See fig. 4.1, 4.2 and 4.3).

4.4 SURFACE TEMPERATURE VARIATION OF KATSINA METROPOLIS

Table 4.6: Statistics of Surface Temperature

	1986 (^{o}C)	1999 (^{o}C)	2014 (^{o}C)
Maximum	24.55	39.11	42.59
Minimum	13.31	25.87	29.47
Mean	20.00	32.27	37.13

Source: Author's analysis of surface temperature (2014)

From table 4.6, it could be seen that the maximum value of ST in 1986 was 24.55^{o}C while the minimum value was 13.31^{o}C. In 1999, the maximum and minimum ST values increased drastically to 39.11^{o}C and 25.87^{o}C respectively. The ST continued to increase in 2014 with a maximum value of 42.59^{o}C and a minimum value of 29.47^{o}C. From this study, the mean values of ST in 1986, 1999 and 2014 were 20^{o}C, 32.27^{o}C and 37.13^{o}C

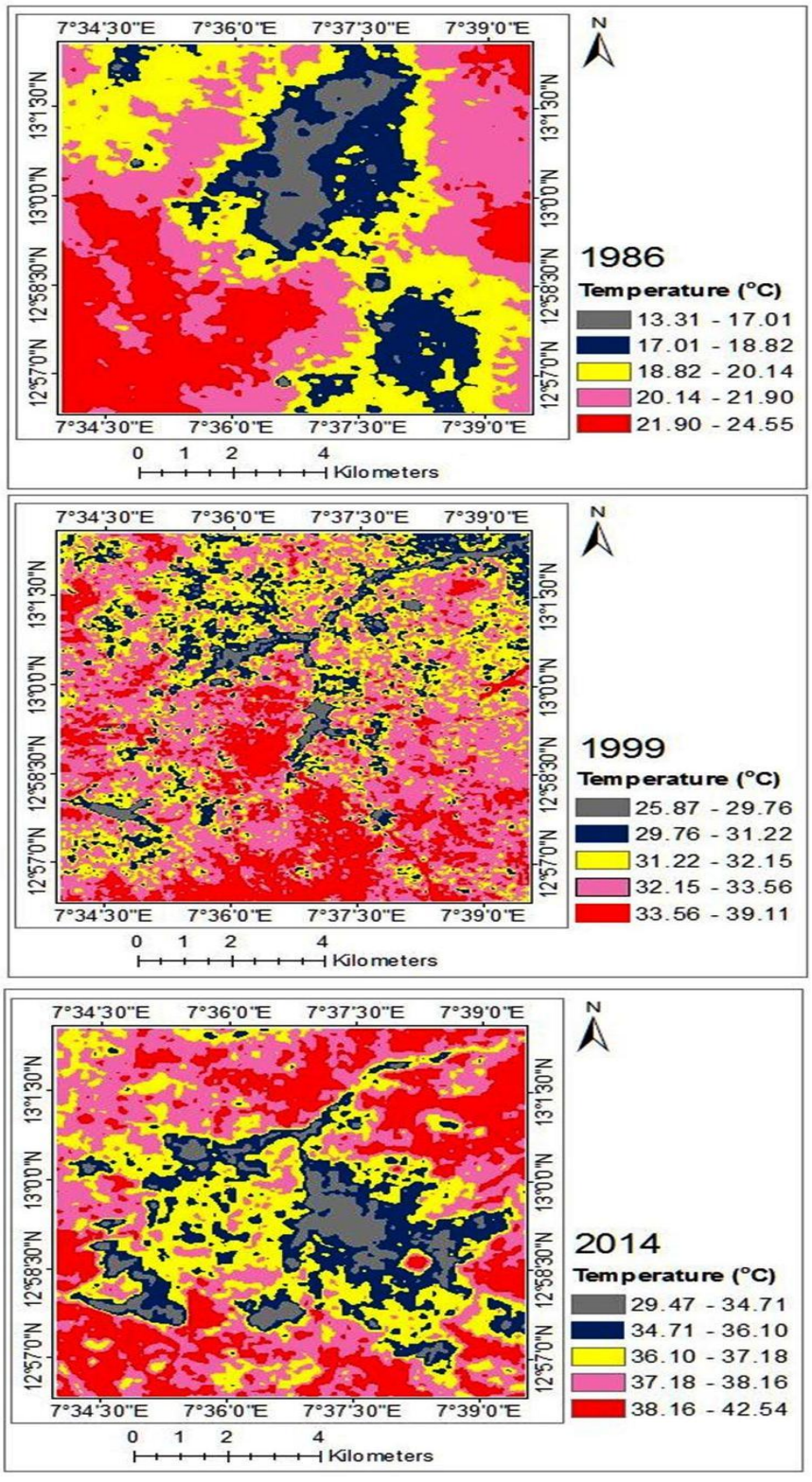


Fig. 4.4: Surface Temperature Map of 1986, 1999 and 2014
Source: Author's analysis of Surface Temperature (2014)

4.5 SURFACE TEMPERATURE OF LAND USE LAND COVER TYPES

Table 4.7 shows the average values of surface temperature (^{o}C) for each of the land use/cover in 1986, 1999 and 2014.

Table 4.7: Surface Temperature Statistics of Land use/cover types

	Average Surface Temperature (^{o}C)		
Class	1986	1999	2014
Built up	19.07	32.87	36.14
Farmland	20.19	31.94	38.15
Vegetation	16.03	28.08	33.41
Bareland	21.81	34.40	39.55

Source: Author's analysis of surface temperature (2014)

From Table 4.7 it is obvious that bareland exhibits the highest surface temperature (21.8^{o}C in 1986, 34.40^{o}C in 1999 and 39.55^{o}C in 2014), followed by farmland (20.19^{o}C in 1986, 31.94^{o}C in 1999 and 38.15 ^{o}C in 2014). In 1986, 1999, and 2014 the values of ST exhibited by built up are 19.07^{o}C, 32.87^{o}C and 36.14^{o}C respectively. The lowest values of ST in this study are exhibited by vegetation (16.03^{o}C in 1986, 28.08^{o}C in 1999 and 33.41^{o}C in 2014).

From 1986 to 1999 the surface temperature of built up, farmland, vegetation and bareland in the study area increased by 13.80^{o}C, 11.75^{o}C, 12.05^{o}C and 12.58^{o}C respectively. Similarly, during 1999 and 2014 the surface temperature of built up, farmland, vegetation and bareland appreciated by 3.27^{o}C, 6.20^{o}C, 5.33^{o}C and5.16^{o}C. This represents a general increase in surface temperature of built up, farmland, vegetation and bareland by 17.06^{o}C, 17.96^{o}C, 17.38^{o}C and 17.74^{o}C respectively during 1986 and 2014.

It is evident from table 4.7 that vegetation had shown considerably low ST during the three periods because dense vegetation can reduce the amount of heat stored in the soil and surface structure through transpiration. These results are in line with the findings of Falahatkar, Hosseini

and Soffianian (2011) study of the relationship between land cover changes and spatial-temporal dynamics of land surface temperature in Isfahan. Bareland and farmland have exhibited relatively higher ST values than other land use land cover because they tend to have sparse or complete absence of vegetation. Land use land cover changes driven by urban growth do have serious consequences on ST of any particular place. The increase in surface temperature may also be attributed to higher amount of insolation or other atmospheric factors which needs to be studied.

CHAPTER 5: SUMMARY, CONCLUSSION AND RECOMMENDATIONS

5.1 INTRODUCTION

This chapter highlights some of the findings of this research and recommendations based on the findings of this work.

5.2 SUMMARY

In this study, an integration of remote sensing and GIS was employed to evaluate the effect of rapid urban growth on temporal variation of surface temperature in Katsina metropolis, Nigeria. Three Landsat TM, ETM+ and OLI/TIRS images of 1986, 1999 and 2014 respectively were utilized. Land use land cover maps were generated using supervised classification. The four (4) land use land cover classes identified in the study area are farmland, vegetation, bareland and built up. The overall classification accuracy for 1986, 1999 and 2014 land use land cover maps are 87%, 91% and 85% respectively. Thermal band data was used to compute surface temperature maps for the three years and the relationship between land use land cover and surface temperature was analyzed. Results from land use land cover maps revealed a notable increase in urban land use/cover between 1986 and 2014. The results also showed that urban land development raised surface temperature by more than 17^{o}C between 1986 and 2014. Bareland exhibited the high values of surface temperature while vegetation showed low values of surface temperature. This study has also demonstrated that the direct effect of urban land use/cover change on one environmental element can cause indirect effects on the other.

5.3 CONCLUSSION

For the past 28 years, Katsina metropolis has been experiencing accelerated urban growth. This study has demonstrated how Landsat data can be used to evaluate the effect of urban growth on surface temperature in Katsina metropolis, Nigeria. Remote sensing and GIS were combined to

examine the effect of urban growth on temporal variation of surface temperature. Findings from this study revealed that there is a general decline in natural surfaces and increase in developed surfaces from 1986 to 2014. The resulting GIS analysis showed that built up is increasing at an annual average rate of 5.1 % while the ST has gone up by more than 17^{o}C during the study period. If the built up continue to increase at the rate mentioned above and vegetation decline at an annual rate of 0.8%, ST will be on the high side and this may bring about urban heat island.

5.4 RECOMMENDATIONS

The variations in surface temperatures of the identified land use/cover types of Katsina metropolis suggest that urban growth is a major factor responsible for land transformation in the study area. The increase in rate of surface temperature has its attendant effects on both the environment and the health of residents. Therefore, planting of trees and vegetation in and around the metropolis should be encouraged to minimize the increase in surface temperatures of the land use/cover types which may also affects the mean surface temperature of Katsina metropolis.

Future research works should focus on integrating GIS and satellite remote sensing with high spectral, spatial and temporal resolution at the local scale to develop urban environmental monitoring. Moreover, research works should draw attention to urban land use modeling and techniques integrating socio-economic data and GIS tools to predicting future pattern of change. Focus should be given to the effect of urban growth and growing impervious surfaces, water pollution and stress, etc.

REFERENCES

Abdulhamed, A., Iguisi, E.O., Ati, O.F., Sawa, B.A. & Nduka, I.C. (2012). Paper No 4: *An Analysis of UCHI Characteristics in Kano Metropolis Nigeria*. ICUC8 – 8th International Conference on Urban Climates, 6th-10th August, 2012, UCD, Dublin Ireland.

Abdulkadir, F.I. (2009). Application of geomatics technology in the analysis of the spatial Growth of Katsina metropolis. Office of the Surveyor-General of the State, Nagogo Road Katsina Nigeria.

Adesina, F.A., Siyanbola, W.O., Okelola, F.O., Pelemo, D.A., Ojo, L.O. & Adegbulugbe, A. O. (1999). Potentials of agroforestry for climate change mitigation in Nigeria, some preliminary estimates. *Journal of Global Ecology Biogeography Letters*, 8, 163-173.

Alkali, J.L.S. (2005). *Planning Sustainable Urban Growth in Nigeria: Challenges and Strategies*. A Paper Presented at the Conference on Planning Sustainable Urban Growth and Sustainable Architecture Held at ECOSOG Chambers, United Nations Headquarters, New York.

Anandakumar, K. (1999). A study on the partition of net radiation into heat fluxes on a dry asphalt surface. *Atmospheric Environment* 33: 3911-3918.

Arrau, C.P. & Pena, M.A. (2010). The Urban Heat Island (UHI) Effect. Retrieved from http://www.urbanheatislands.com.

Ayedun, C.A., Durodola, O.D. & Akinjare, O.A. (2011). Towards ensuring sustainable urban growth and development in Nigeria: Challenges and Strategies. *Business Management Dynamics*, 1(2), 99-104. Retrieved from www.bmdynamics.com.

Babsal, A.K. (1998). Katsina State Environmental Action Plan (KATSEPA). Federal Republic of Nigeria.

Balogun, I.A., Adeyewa, D.Z., Balogun, A.A. & Morakinyo, T.E. (2011). Analysis of expansion and land use changes in Akure, Nigeria using remote sensing and geographic information system (GIS) techniques. *Journal of Geography and Regional Planning* 4(9) 533-541. Retrieved from http://www.academicjournal.org/JGRP

Bhatta, B. (2009). Modelling of urban growth boundary using geoinformatics. *International Journal of Digital Earth*, 2(4), 359–381.

Bhatta, B. (2010). *Analysis of Urban Growth and Sprawl from Remote Sensing Data*, Advances in Geographic Information Science, DOI 10.1007/978-3-642-05299-6_2, Springer-Verlag Berlin Heidelberg.

Bernstein, M. & Whitman, D. (2005). The challenges of battling ozone formation.

Berry, P., Richters, K., Clarke, K. & Brisbois, M. (2011). Assessment of Vulnerability to the Health Impacts of Extreme Heat in the City of Windsor. Ottawa: Health Canada.

Bowler, D.E., Buyung-Ali, L., Knight, T.M. & Pullin, A.S. (2010). Urban greening to cool towns and cities: A systematic review of the empirical evidence. *Landscape and Urban Planning, 97*(1), 147- 155.

Boyce, R.R. (1963). Myth versus reality in urban planning. Land Economics, 39(3), 241–251.

Brookfield, H. & Byron, Y. (1993). South-East Asia's Environmental Future: The Search for Sustainability. Kuala Lumpur: Oxford University Press and United Nations University Press.

Brun, S.E. & L.E. Band, (2000). Simulating runoff behavior in an urbanizing watershed, Computers, Environment and Urban Systems, 24:5–22.

Burchell, R.W., Downs, A., McCann, B. & Mukherji, S. (2005). *Sprawl Costs: Economic Impacts of Unchecked Development*. Island Press, Washington, DC.

Campbell, J.B. (2002). Introduction to Remote Sensing, 3rd edition, The Guilford Press, New York, New York, 621 p.

Carnahan, W.H. & Larson, R.C. (1990). An analysis of an urban heat sink, *Remote Sensing of Environment*, 33:65–71.

Caselles, V., LopezGarcia, M.J., Melia, J., & PerezCueva, A.J. (1991). Analysis of the heat-island effect of the city of Valencia, Spain through air temperature transets and NOAA satellite data. Theoretical and Applied Climatology, 43, 195– 203.

Caselles, V., Sobrino, J.A. & Coll, C. (1992). A physical model for interpreting the land surface temperature obtained by remote sensors over incomplete canopies. *Remote Sensing of Environment,* 39, 203– 211.

Chan, C.F., Lebedeva, J., Otero, J. & Richardson, G. (2007). Urban Heat Island: A Climate Change Adaptation Strategy for Montreal. Retrieved from http://www.mcgill.ca/files/urbanplanning/CCAPUHIFinalReport-2007.pdf.

Chen, X.L., Zhao, H.M., Li, P.X. &Yin, Z.Y. (2006). Remote sensing image-based analysis of the relationship between urban heat island and land use/cover changes. *Journal of Remote Sensing of Environment,* 104, 133-146.

Chiesura, A. (2004). The role of urban parks for the sustainable city. *Landscape and Urban Planning*, Vol. 68, No. 1, pp. 129-138.

Clapham, W.B. (2003). Continuum-based classification of remotely sensed imagery to describe urban sprawl on a watershed scale, *Remote Sensing of Environment*, 86:322–340.

Danbuzu, L.A.S. (2012). Spatial Distribution of Solid Waste Collection Points in Urban Katsina, Northern Nigeria. An Unpublished M.Sc Thesis Submitted to the Department of Geography Bayero University, Kano Nigeria.

Dash, P., Göttsche, F.M., Olesen, F.S. & Fischer, H. (2002): Land surface temperature and emissivity estimation from passive sensor data: Theory and practice-current trends. *International Journal of Remote Sensing,* 23, 2563-2594.

DeCarolis L. (2012). The Urban Heat Island Effect in Windsor, ON: An Assessment of Vulnerability and Mitigation Strategies. Report Prepared for the City of Windsor August, 2012.

DelBarrio, E.P. (1998). Analysis of the green roofs cooling potential in buildings. *Energy and Buildings* 27: 179–193.

Doygun, H. & Ilter, A.A. (2007). Investigating Adequacy of Existing and Proposed Active Green Spaces in Kahramanmaras City. *Ekoloji* 17 (65), 21-27.

Duprax, C. (1994). Prospects for easing land tenure conflicts with Agroforestry in Mediterranean France. A research approach for inter cropped timbers orchards. Agroforestry systems. 25 (3): 181.

Ehlers, M., Jadkowski, M.A., Howard, R.R. & Brostuen, D.E. (1990), Application of SPOT data for regional growth analysis and local planning. *Journal of Photogrammetric Engineering and Remote Sensing*, 56, 175–180.

Environment Canada. (2010). *Natural Gas Fired Power. Available at* http://www.ec.gc.ca/energie-energy/default.asp?lang=En&n=7ED2A11B-1

Environmental Protection Agency. (2008). Reducing Urban Heat Islands: Compendium of Strategies. Washington, DC: United States Environmental Protection Agency.

Environmental Protection Agency, (2009). Reducing Urban Heat Islands: Compendium of Strategies – Urban Heat Island Basics. Retrieved from http://www.epa.gov/heatisland/resources/pdf/BasicsCompendium.pdf

Falahatkar, S., Hosseini, S.M. & Soffianian, A.R. (2011). The relationship between land cover changes and spatial-temporal dynamics of land surface temperature. *Indian Journal of Science,* 4 (2), 76-80. Retrieved from http://www.indjst.org.

Fasal, S. (2000). Urban expansion and loss of agricultural land- A GIS based study of Saharanpur City, India. *Journal of Environment and Urbanisation*, 12(2), 133-149.

Forkes, J. (2010). Urban Heat Island Mitigation in Canadian Communities. Toronto, ON: Clean Air Partnership.

Frumkin, H. (2002). Urban sprawl and public health. *Public Health Reports*, 117, 201–217.

Gide, Y. (2012). *Impact of Urban Growth on the Microclimate of Katsina Metropolis.* A published M. Sc thesis, submitted to the Department of Geography A.B.U – Zaria.

Giuliano, G. (1989). Literature Synthesis: Transportation and Urban Form. Report prepared for the Federal Highway Administration under Contract DTFH61-89-P-00531.

Global Cool Cities Alliance. (2012). Cool Roofs and Cool Pavements Toolkit. Retrieved from http://www.coolrooftoolkit.org/read-the-guide.

Goward, S.N. (1981). Thermal behaviour of urban landscapes and the urban heat island. Physical Geography, *Remote Sens. Environ*. 2:19-33.

Goward, S.N., Xue, Y. & Czajkowski, K.P. (2002). Evaluating land surface moisture conditions from the remotely sensed temperature/vegetation index measurements: An exploration with the simplified simple biosphere model. *Remote Sensing of Environment*, 79, 225– 242.

Grimmond C.S.B. (2007). Urbanization and global environmental change: local effects of urban warming. *The Geographical Journal,* 173: 83-88.

Harvey, R.O. & Clark, W.A.V. (1965). The nature and economics of urban sprawl. Land Economics, 41(1), 1–9.

Hassan, A. (2008). Analysis of Household Energy Utilization in Katsina Metropolis. An Unpublished M.Sc Thesis submitted to the Department of Geography, Bayero University, Kano.

Health Canada. (2006). Environmental and Workplace Health: Let's Talk About Health and Air Quality. Retrieved from http://www.hc-sc.gc.ca/ewh-semt/air/out-xt/effe/talk-a_propos-eng.php#sulphur.

Health Canada. (2011). Adapting to Extreme Heat Events: Guidelines for Assessing Health Vulnerability. Ottawa, ON: Health Canada.

Heisler, G.M., Grimmond, S., Grant, R.H. & Souch, C. (1994). Investigation of the influence of Chicago's urban forests on and air temperature within residential neighborhoods. *Northeaster Forest Experiment,* Vol. 186, pp. 19-40.

Health Scotland, greenspace scotland, Scottish Natural Heritage & Institute of Occupational Medicine. (2008). *Health impact assessment of greenspace: a guide*. Greenspace Scotland, Stirling, 74 p.

Herb, W.R., Janke, B., Mohseni, O. & Stefan, H.G. (2008) Ground surface temperature simulation for different land covers. *Journal of Hydrology*, 356: 327-343.

Houston Advanced Research Center. (2009). Dallas Urban Heat Island – Sustainable Skylines Initiative. Retrieved from http://files.harc.edu/Projects/DallasUHI/FinalReport.pdf.

Hung, T., Uchihama, D., Ochi, S. & Yasuoka, Y. (2006). Assessment with satellite data of the urban heat island effects in Asian mega cities, *International Journal of Applied Earth Observation and Geoinformation,* 8, pp. 34–48

Jacquin, A., Misakova, L. & Gay, M. (2008). A hybrid object-based classification approach for mapping urban sprawl in periurban environment. *Landscape and Urban Planning*, 84, 152–165.

Kaya, S., Basar, U.G., Karaca, M. & Seker, D.Z. (2012). *Assessment of Urban Heat Islands Using Remotely Sensed Data Ekoloji* 21(84), 107-113.

Kotani, A. & Sugita, M. (2005). Seasonal variation of surface fluxes and scalar roughness of suburban land covers. *Agricultural and Forest Meteorology,* 135: 1–21.

Landsat 7 Science Data User's Handbook (2002). Goddard Space Flight Center, NASA, Washington, DC. Retrieved from http://ltpwww.gsfc.nasa.gov/IAS/handbook/handbook_toc.html

Larson, R.C. & Carnahan, W.H. (1997). The influence of surface characteristics on urban radiant temperatures, *Geocarto International*, 12:5–16.

McPherson, G., Simpson, J.R., Peper, P.J., Mco, S.E. & Siao, Q. (2005) Municipal forest benefits and costs in Five US Cities, *Journal of Forestry*, Vol. 103, No. 8, pp. 411-416.

Meyn, S.K. & Oke, T.R. (2009) Heat fluxes through roofs and their relevance to estimates of urban heat storage. *Energy and Buildings* 41: 745-752.

MLSK (Ministry of Land and Survey, Katsina) (2008): History and Master Plan of Urban Katsina; Survey Department. Katsina: Government Printing Press.

Morris, C.J., Simmonds, I. & Plummer, N. (2001). Quantification of the influences of wind and cloud on the nocturnal urban heat island of a large city. *Journal of Applied Meteorology, 40*(2), 169-181.

Nichol, J.E. (1996). High-resolution surface temperature patterns related to urban morphology in a tropical city: A satellite-based study, *Journal of Applied Meteorology*, 35:135–146.

Oguntoyinbo, J.S. (1984). Some Aspect of the Urban Climate of Tropical Africa. Urban climatology and its applications with special regard to tropical areas. WMO No. 652, 110 – 132.

Oke, T.R. (1987). Boundary layer climates. 2nd ed., Routledge, London & New York: 435pp.

Oke, T.R. (1982). The energetic basis of the urban heat island, *Quarterly Journal of the Royal Meteorological Society*, 108:1–24.

Ologe, K.O. (1985). An Atlas of Structural Landforms in Nigeria. An Occasional Paper, 9, Geography Department, Ahmadu Bello University, Zaria.

Owen, T.W., Carlson, T.N. & Gillies, R.R. (1998). An assessment of satellite remotely-sensed land cover parameters in quantitatively describing the climatic effect of urbanization. *International Journal of Remote Sensing*, 19, 1663– 1681.

Patz, J., Campbell-Lendrum, D., Holloway, T. & Foley, J.A. (2005). Impacts of regional climate change on human health. *Nature, 438*(17), 310-318.

Prata, A.J., Caselles, V., Coll, C., Sobrino, J.A. & Ottlé, C. (1995): Thermal remote sensing of land surface temperature from satellites: Current status and future prospects. Remote Sensing Reviews 12, 175-224.

Quattrochi, D.A. & Luvall, J.C. (1999). Thermal infrared remote sensing for analysis of landscape ecological processes: Methods and applications. *Journal of Landscape Ecology*. 14(6), 577-598.

Rail, A.N. (2007). *Urban thermal plumes, their possible impact on climate change*. Kastell Books, Sudbury, Suffolk.

Rizwan, A.M., Dennis, L.Y. & Chunho, L. (2008). A review of the generation, determination and mitigation of urban heat islands. *Journal of Environmental Sciences*, 20(1), 120-128.

Rao, P.K. (1972). Remote sensing of urban heat islands from an environmental satellite. *Bulletin of the American Meteorological Society*, 53, 647– 648.

Roa-Espinosa, A., Wilson, T.B., Norman, J.M. & Johnson, K. (2003). *Predicting the impact of urban development on stream temperature using a thermal urban runoff model.* Retrieved from http://www.epa.gov/owow/NPS/natlstormwat er03/31.

Rosenzweig, C., Solecki, W. & Slosberg, R. (2006). *Mitigating New York City's Heat Island with Urban Forestry, Living Roofs, and Light Surfaces.* Albany, NY: New York State Energy Research and Development Authority.

Rossi, L. & Hari, R.E. (2007). Screening procedure to assess the impact of urban stormwater temperature to populations of brown trout in receiving water. *Integrated Environmental Assessment and Management, 3*(3), 383-392.

Roth, M. (2008). Urban Climate Considerations for the Development of Sustainable Cities. In: *Proceedings for Recent Findings on Planning and Designing Sustainable Cities, Singapore, November 2008.* National University of Singapore. Retrieved from http://www.sde.nus.edu.sg/csac/data/WII%20Asso%20Prof%20Matthias%20Roth.pdf.

Rowntree, R.A. & Nowak, D.J. (1991) Quantifying the role of urban forests in removing atmospheric carbon dioxide, *J. Arboric.*, Vol. 17, pp. 269-275.

Rumah, M.M. & Sheik, A.U. (2010). Reuse of waste water in urban farming and urban planning impliocations in Katsina metropolis, Nigeria. African journal of Environmental Science and Technology, 4(1) 28-33. Retrieved from http://www.academicjournal.org/AJEST

Sailor, D.J. (1995). Simulated urban climate response to modifications in surface albedo and vegetative cover, *Journal of Applied Meteorology*, 34(7), 1694–1704.

Sailor, J. (2008). A green roof model for building energy simulation programs. *Energy and Buildings* 40: 1466–1478.

Saleh, A.H.S. (2010). *Impact of urban expansion on surface temperature in Baghdad, Iraq using remote sensing and GIS techniques*, 13(1), 48-59.

Santana, L.M. (2007). Landsat ETM+ image applications to extract information for environmental planning in a Colombian city. *International Journal of Remote Sensing*, 28, 4225-4242.

Scherba, A., Sailor, D.J., Rosenstiel, T.N. & Warnser, C.C. (2011) Modeling impacts of roof reflectivity, integrated photovoltaic panels and green roof systems on sensible heat flux into the urban environment. *Building and Environment* 46: 2542-2551.

Scholz, M. & Grabowiecki, P. (2007). Review of permeable pavement systems. *Building and Environment, 42*(1), 3830-3836.

Shimoda, Y. (2003). Adaptation measures for climate change and the urban heat island in Japan's built environment. *Building Research & Information, 31*(4), 222-230.

Solecki, W.D., Rosenzweig, C., Pope, G., Parshall, L. & Wiencke, M. (2003). *The Current and Future Urban Heat Island Effect and Potential Mitigation Strategies in Greater Newark, New Jersey Region.* Retrieved June 18, 2012, from, www.cleanairpartnership .org/pdf/finalpaper_solecki.pdf.

Singh, A. (1989). Digital change detection techniques using remotely sensed data. *International Journal of Remote Sensing* 10(6):989-1003.

Solecki, W.D., Rosenzweig, C., Parshall, L., Pope, G., Clark, M., Cox, J. & Wiencke, M. (2005). Mitigation of the heat island effect in urban New Jersey. *Global Environmental Change Part B: Environmental Hazards,* Vol. 6, No. 1, pp. 39-49.

Stone, B., Hess, J.J. & Frumkin, H. (2010). Urban form and extreme heat events: Are sprawling cities more vulnerable to climate change than compact cities? *Environmental Health Perspectives, 118*(10), 1425-1428.

Stathopoulou, M., Cartalis, C. & Petrakis, M. (2007). Integrating Corine Land Cover data and Landsat TM for surface emissivity definition: application to the urban area of Athens, Greece. *International Journal of Remote Sensing*, 28, 3291-3304.

Stutz, F.P. & DeSouza, A.R. (1998). *The World Economy*. Upper Saddle River, New Jersey: Prentice Hall.

Sundseth, K. & Raeymaekers, G. (2006). Biodiversity and natura 2000 in urban areas, nature in cities across Europe: a review of key issues and experiences. IBGE/BIM, Bruxelles, 70 p.

Taha, H., Konopacki, S. & Gabersek, S. (1996). Modeling the meteorological and energy effects of urban heat islands and their mitigation: a 10 region study, report *LBNL-44222, Lawrence* Berkeley National Laboratory, Berkeley, CA., 51 p.

Takebayashi, H. & Moriyama, M. (2012). Research article study on surface heat budget of various pavements for urban heat island mitigation. *Advances in Materials Science and Engineering*, Article ID 523051.

Treitz, P.M., Howard, P.J. & Gong, P. (1992). Application of satellite and GIS technologies for land-cover and land-use mapping at the rural-urban fringe: a case study. *Journal of Photogrammetric Engineering and Remote Sensing*, 58, 439–448.

Tyubee, B.T. & Anyadike, R.N.C. (2012). Analysis of Surface Urban Heat Island in Makurdi, Nigeria.

Unger, J., Sumeghy, Z. & Zoboki, J. (2001). Temperature cross-section features in an urban area*, Atmospheric Research*, 58, 117-127.

UN-Habitat (2012). State of the World's Cities Report, World Urban Forum edition, Nairobi, Kenya. Retrieved from http://www.unhabitat.org.

Van-Tijen, M. & Cohen, R. (2008). Features and benefits of cool roofs: The cool roof rating council program. *Journal of Green Building, 3*(2), 13-20.

Voogt, J.A. & Oke, T.R. (2003). Thermal Remote Sensing of Urban Areas. *Remote Sensing of Environment* 86: 370−384.

Voogt, J. (2002). Urban Heat Island. In Munn, T. (ed.) *Encyclopedia of Global Environmental Change*, Vol. 3. Chichester: John Wiley and Sons.

Weng, Q. (2001). A remote sensing–GIS evaluation of urban expansion and its impact on surface temperature in the Zhujiang Delta, China. *International Journal of Remote Sensing*, 22(10), 1999-2014. Retrieved from http://www.tandf.co.uk/journals.

Weng, Q. (2009). Thermal infrared remote sensing for urban climate and environmental studies: Methods, applications, and trends. *ISPRS Journal of Photogrammetry and Remote Sensing,* 64, 335–344.

Wisner, B., Blaikie, P., Cannon, T. & Davies, I. (2004). At Risk, Natural Hazards, People's Vulnerability and Disasters. Routlegde, London, p. 471.

Wilhelmi, O.V., Purvis, K.L. & Harriss, R.C. (2004). Designing a geospatial information infrastructure for mitigation of heat wave hazards in urban areas. *Natural Hazards Review, 5*(3), 147- 158.

Yang, X. (2013). Temporal variation of urban surface and air temperature. A published thesis submitted in partial fulfillment of the requirements for the degree of Doctor of philosophy at the depatment of Mechanical engineering, the university of Hong kong.

Yow, D.M. (2007). Urban heat islands: Observations, impacts, and adaptation. *Geography Compass, 1*(6), 1227-125

Yuan, F. & Bauer, M.E. (2007). Comparison of impervious surface area and normalized difference vegetation index as indicators of surface urban heat island effects in Landsat imagery. *Remote Sensing of Environment*, 106, 375-386.

Yue, W., Xu, J., Tan, W. & Xu, L. (2007). The relationship between land surface temperature and NDVI with remote sensing: application to Shanghai Landsat 7 ETM+ data. *International Journal of Remote Sensing*, 28, 3205-3226.

Zayyana, Y.I. (2010). Some Aspects of Urban Farming in Urban Katsina, Katsina State. An unpublish M.Sc Thesis Submitted to the Department of Geography, Bayero University, Kano.

Zemba, A.A., Adebayo, A.A. & Musa, A.A. (2010). Evaluation of The Impact of Urban Expansion on Surface Temperature Variations Using Remote Sensing-GIS Approach. *Global Journal of Human Social Science*, 10, 2.

Zhang, Z. & He, G. (2006). A study on urban growth, vegetation space variation and thermal environmental changes of Beijing city based on TM imagery data. *Proceedings of the 2nd WSEAS International Conference on Remote Sensing*, Tenerife, Canary Islands, Spain